

Lattice Chiral Fermion without Hermiticity

Chen-Te Ma^{a,b,c,d,e,f}¹ and Hui Zhang^{c,e,g,h}²

^a *Department of Physics and Astronomy, Iowa State University, Ames, Iowa 50011, US.*

^b *Asia Pacific Center for Theoretical Physics, Pohang University of Science and Technology, Pohang 37673, Gyeongsangbuk-do, South Korea.*

^c *Guangdong Provincial Key Laboratory of Nuclear Science, Institute of Quantum Matter, South China Normal University, Guangzhou 510006, Guangdong, China.*

^d *School of Physics and Telecommunication Engineering, South China Normal University, Guangzhou 510006, Guangdong, China.*

^e *Guangdong-Hong Kong Joint Laboratory of Quantum Matter, Southern Nuclear Science Computing Center, South China Normal University, Guangzhou 510006, China.*

^f *The Laboratory for Quantum Gravity and Strings, Department of Mathematics and Applied Mathematics, University of Cape Town, Private Bag, Rondebosch 7700, South Africa.*

^g *Key Laboratory of Atomic and Subatomic Structure and Quantum Control (MOE), Guangdong Basic Research Center of Excellence for Structure and Fundamental Interactions of Matter, Institute of Quantum Matter, South China Normal University, Guangzhou 510006, China.*

^h *Physics Department and Center for Exploration of Energy and Matter, Indiana University, Bloomington, Indiana 47408, US.*

¹e-mail address: yefgst@gmail.com

²e-mail address: Mr.zhanghui@m.scnu.edu.cn

Abstract

Our review of the lattice chiral fermion delves into some critical areas of lattice field theory. By abandoning Hermiticity, the non-Hermitian formulation circumvents the Nielsen-Ninomiya theorem while maintaining chiral symmetry, a novel approach. Comparing the Wilson and overlap fermions gives insight into how lattice formulations handle chiral symmetry. The Wilson fermion explicitly breaks chiral symmetry to eliminate doublers. In contrast, the overlap fermion restores a modified form of chiral symmetry using the Ginsparg-Wilson relation. We investigate how the (1+1)D Wilson fermion relates to the (1+1)D overlap fermion in the Hamiltonian formulation. This connection could provide a clearer physical understanding of how chiral symmetry manifests at the lattice level. Depending on Hermiticity for efficiency, Monte Carlo methods face unique challenges in a non-Hermitian setting. We investigate how to correctly apply this method to non-Hermitian lattice fermions, which is essential for practical simulations. Finally, the review of topological charge is crucial, as topological features in lattice formulations are strongly connected to chiral symmetry, anomalies, and the index theorem.

1 Introduction

Lattice field theory indeed provides a robust framework for *non-perturbative* solutions to quantum field theory (QFT) [1]. The method, introduced by Wilson, replaces continuous spacetime with a discrete lattice, regularizing QFT [2] by introducing a natural cutoff—the lattice spacing—avoiding infinities that occur in the continuum path integral formulation [1]. In the continuum limit, where the lattice spacing tends to zero, and the lattice size becomes infinite, the theory should ideally converge to the desired continuum QFT [1].

One of the critical aspects of lattice field theory is that it makes renormalization possible in a non-perturbative setting by implementing the renormalization group (RG) [3] on a discrete space. However, the connection between lattice computations and the continuum limit involves subtle issues. The RG flow on the lattice may make it challenging to determine whether a lattice theory recovers the correct physics of the continuum theory. For example, certain symmetries, such as chiral symmetry, are difficult to realize on the lattice without introducing either fermion doublers (as per the Nielsen–Ninomiya theorem) [4, 5] or using non-local operators (such as in overlap fermions) [6]. Furthermore, the presence of lattice artifacts due to the finite lattice spacing requires careful extrapolation to the continuum limit, which can introduce computational challenges. While lattice field theory regularizes QFT and simplifies numerical simulations, ensuring that the results correspond to physical continuum observables requires careful consideration of RG flows and lattice artifacts. The problem is exceptionally intricate for theories with massless fermions or when maintaining chiral symmetry is crucial, as demonstrated by the developments around Wilson [1] and overlap fermions.

Nielsen–Ninomiya theorem imposes significant constraints on lattice fermion formulations by showing that under certain conditions—namely, Hermiticity, locality, and chiral symmetry—it is impossible to avoid the fermion doubling problem when transitioning from a lattice to the continuum theory [7]. This implies that, under these assumptions, lattice fermions will always include multiple unwanted species (doubblers), which is problematic for simulating models like the Standard Model. To overcome this, different approaches relax one or more of these conditions:

- Wilson fermions solves the doubling problem by explicitly breaking chiral symmetry. A term is added to the lattice action that suppresses the doublers. However, it introduces chiral symmetry breaking at *finite* lattice spacing, which needs to

be carefully restored in the continuum limit.

- Overlap fermions are based on the Ginsparg-Wilson relation [8], which modifies the concept of chiral symmetry on the lattice [9]. Overlap fermions preserve a modified version of chiral symmetry [9] and can avoid doublers. However, they involve nonlocal operators [10], making them more computationally intensive.

In our exploration of non-Hermitian formulations [11], it is interesting to consider how the relaxation of Hermiticity might allow different ways of dealing with fermion doubling and chiral symmetry without needing to follow the traditional paths of Wilson or overlap fermions.

We highlight an exciting connection between Wilson and overlap fermions, especially in (1+1)D Hamiltonian formulation [12, 13]. The fact that on a finite lattice, the Wilson fermion formulation becomes equivalent to the overlap fermion formulation [14] suggests that certain lattice artifacts, typically problematic in lattice field theory, might manifest modified symmetries that reflect the underlying continuum symmetries. This equivalence implies that the modified chiral symmetry of overlap fermions, which was introduced to bypass the no-go theorem (Nielsen-Ninomiya), also appears in the Wilson fermion formalism in such constrained scenarios. This discovery is insightful when exploring the broader symmetry structure of lattice field theories. Since symmetries often dictate much of the physical content in lattice and continuum formulations, realizing a typical symmetry between two formulations is significant. It hints that new lattice symmetries could be at play, possibly beyond the familiar continuum analogs, offering a pathway to further understanding how continuum physics can emerge cleanly from the lattice. In particular, modified chiral symmetry on the lattice via the Ginsparg-Wilson relation in the overlap fermion case shows how lattice symmetries can evolve to include continuum-like behavior without directly imposing it. Suppose this modified symmetry can be extended or generalized under certain conditions in the Wilson fermion formalism. In that case, it could lead to the discovery of more exotic symmetries inherent to the lattice regularization itself. The (1+1)D case is a natural starting point for this exploration. However, extending these ideas to higher dimensions would be fascinating, potentially opening new avenues for both analytic and numerical investigation.

We dive into the subtle interplay between lattice regularization, chiral symmetry, and topological aspects, mainly through the lens of the Ginsparg-Wilson relation and its implications for *topological charge* and *zero modes*. Finite lattices introduce artifacts

that can break the symmetries of the underlying continuum theory. Preserving these symmetries on the lattice improves the correspondence with the continuum, which is essential for analyzing numerical simulations. However, a finite lattice generally depends on the lattice spacing, making preserving topological properties challenging. The Atiyah-Singer index theorem connects the zero modes of the Dirac operator D with the topological charge of the background gauge field [15, 16, 17]. On the lattice, this theorem is non-trivial due to the discretization process [18]. Nevertheless, efforts have been made to formulate the index theorem for lattice systems, especially in light of Ginsparg-Wilson fermions, which maintain a modified chiral symmetry. By integrating out the fermion fields, one obtains a Jacobian that relates to the anomaly structure [19] and the lattice index theorem [20, 21, 22]. This approach helps formulate a lattice version of the index theorem. Topological zero modes in the Dirac operator are a hallmark of topologically non-trivial gauge field backgrounds in the continuum. However, on the lattice, the Ginsparg-Wilson relation does not always guarantee the presence of topological zero modes [23] or a non-trivial topological charge [24]. This is due to the loss of the winding part of the topological charge density in the transition from the lattice to the continuum, even if the smooth part is recovered [25]. While the other part of the topological charge density can be recovered from topologically non-trivial gauge fields, the non-trivial contribution to the topological charge comes from the winding part [25]. This means that a lattice Dirac operator does not exhibit topological zero modes in such backgrounds [25]. While topological zero modes lack experimental evidence, the topological charge density has observable consequences, making it a more direct physical observable [25]. The subtlety arises from the fact that the topological charge density and zero modes are related in theory. However, the lattice formulation introduces complexities that decouple them in some cases. In essence, we highlight how lattice formulations, particularly via the Ginsparg-Wilson relation, strive to capture continuum topological features. However, lattice artifacts and the system's finite nature create challenges in preserving the full topological structure, particularly in terms of zero modes and charge densities. This remains an area of ongoing study and refinement.

The use of *one-sided* lattice differences in the non-Hermitian formulation *breaks* Hermiticity, which complicates conventional approaches to lattice fermion formulations [11]. This *breaking* of hypercubic symmetry means that the theory loses renormalizability in the standard sense, and physical observables should become dependent on the lattice spacing [11]. Non-physical poles in the propagator *decouple* in the continuum limit, leading to consistent particle descriptions as the spacing vanishes [11]. The loss of

hypercubic symmetry at the lattice level can be addressed by performing a *quenched averaging* over all directions in the space [11]. This restores the symmetry at the level of the observables, as noted in 4D quantum electrodynamics (QED) studies, such as those in the weak-coupling expansion [26]. One key issue is that Monte Carlo simulations rely on a positive definite partition function, *not* necessarily on Hermiticity in the Lagrangian [27]. Introducing pseudo-fermion fields and considering fermions with one-sided differences in opposite directions can rewrite the theory to yield a positive definite partition function, making Monte Carlo (MC) simulations applicable [27]. This method has been demonstrated for free Dirac fermions [27] and in models like the 2D Gross-Neveu-Yukawa (GNY) model [28]. Such an implementation is similar to investigating the Quantum Chromodynamics (QCD) phase diagram with opposite isospin chemical potential [29]. The non-Hermitian formulation maintains chiral symmetry exactly, which leads to exciting properties regarding the index theorem. The *bi-orthogonal* basis is introduced to realize the index theorem in a non-Hermitian setting [30]. However, the *absence* of non-trivial topological charge, as seen in Hermitian formulations due to the exact chiral symmetry [31], is a significant consequence [27, 31]. Despite the complexities introduced by the lack of Hermiticity, the non-Hermitian approach offers computational advantages. For example, since the method *avoids* non-local operators, it can reduce simulation time. Furthermore, preserving chiral symmetry at the lattice level provides convenience in analyzing the numerical result.

The motivation for using lattice field theory is to study interacting field theories, particularly in the context of ultraviolet (UV) completeness and non-perturbative effects. If a theory is not UV complete, the RG flow's consistency leads to triviality, implying the coupling vanishes [32, 33]. Therefore, the practical application of lattice theory requires consideration of a UV complete theory. Lattice QCD is a prominent example, where the asymptotic freedom of quarks and gluons at high energy scales [34, 35] justifies the use of lattice techniques. The 2D GNY model also provides an excellent playground for investigating asymptotic safety, which was confirmed by the bosonization techniques (one flavor) [36, 37, 38, 39, 40, 41, 42, 43, 44] and the lattice simulation and the resummation (two flavors) [28].

Lattice field theory is influential because it allows for non-perturbative calculations that are difficult to achieve using other techniques. Resummation methods [45, 46] and lattice simulations all play roles in understanding field theory beyond perturbation theory. However, the continuum limit remains a central challenge in lattice formulations,

as correctly describing the original QFT without lattice artifacts is necessary.

The comparison between lattice results and non-perturbative resummation techniques highlights the importance of carefully examining non-perturbative phenomena. In some cases, lattice methods can provide insights into invisible effects in perturbative expansions or requiring extensive resummation. Balancing these methods to cross-check and validate results is essential, especially when studying models like the 2D GNY model where asymptotic safety or other non-perturbative behaviors are of interest.

1.1 Outline

The outline of this review is as follows. We introduce the path integral approach and its application in QFT in Sec. 2 and the RG flow in Sec. 3. The essential concepts of QFT related to the lattice field theory are covered.

We discuss the difficulties of putting the chiral fermions on a lattice and the various lattice constructions in Sec. 4. It includes the challenges of defining chiral fermions on the lattice, including the Nielsen–Ninomiya theorem and the fermion doubling problem. We review solutions like Wilson fermions, overlap fermions, and non-Hermitian formulations that circumvent the no-go theorem.

We present numerical methods for simulating lattice fermions in Sec. 5. It includes discussions on the Metropolis and Hybrid MC algorithms and the conjugate gradient method, which is the most time-consuming part of simulating lattice fermions. We discuss the chiral anomaly and the index theorem in Sec. 6. It includes details about realizing the index theorem on the lattice, focusing on the Ginsparg-Wilson relation. This section also includes connecting topological zero modes and non-trivial gauge backgrounds. We outline potential research areas that could advance the study of lattice chiral fermions in Sec. 7.

2 Path Integral Formulation

We review the path integral formulation from the operator formulation. We then provide an explicit example with a velocity-dependent potential to demonstrate the path integral formalism. The subtlety of a measure is demonstrated in the finite temperature case, which is introduced by a Wick rotation. We use the 0D QFT to show the neces-

sity of the non-perturbative effect that the weak-coupling perturbation cannot reach. Ultimately, we introduce the path integral formulation for the fermion fields.

2.1 From Operator Formalism to Path Integral Formalism

We first derive the path integration formalism in 1D QFT. In the path integral formalism, we use the Heisenberg picture. The Heisenberg picture state $|x, t\rangle_H$ is an eigenstate of the Heisenberg picture position operator $X_H(t)$:

$$\hat{X}_H(t)|x, t\rangle_H \equiv x|x, t\rangle_H; \quad \hat{X}_H(t) = e^{i\hat{H}t}\hat{X}_S e^{-i\hat{H}t}, \quad (1)$$

where \hat{X}_S is the time independent position operator, and \hat{H} in the exponent is Hamiltonian. The Schrödinger picture state is related to the Heisenberg picture state in the following way:

$$|x\rangle_S = e^{-i\hat{H}t}|x, t\rangle_H; \quad |x\rangle_H = e^{i\hat{H}t}|x, t\rangle_S, \quad (2)$$

which is an eigenstate of the Schrödinger picture position operator

$$\hat{X}_S|x\rangle_S = x|x\rangle_S. \quad (3)$$

Because we want to show how operators become a classical variable in a path integral formalism, we use $\hat{\cdot}$ to label an operator for distinguishing operators and classical variables.

In classical mechanics, the momenta and position operators do not have an ambiguity for ordering, but lifting classical variables to quantum operators does. The issue is due to the commutation relation

$$[\hat{p}, \hat{x}] = -i. \quad (4)$$

A classical Hamiltonian is

$$H(p, q) = f_{ab}p^a q^b, \quad (5)$$

and then a canonical quantization gives:

$$x \rightarrow \hat{x}, \quad p \rightarrow \hat{p} \quad (6)$$

with the commutation relation. The quantum Hamiltonian is not unique like the following:

$$\hat{H}_L \equiv f_{ab}\hat{p}^a\hat{x}^b; \quad \hat{H}_R \equiv f_{ab}\hat{x}^b\hat{p}^a. \quad (7)$$

We select either a Weyl ordering or a symmetric ordering

$$(\hat{x}\hat{p})_W \equiv \frac{1}{2}(\hat{p}\hat{x} + \hat{x}\hat{p}) \quad (8)$$

for obtaining a hermitian Hamiltonian. The transition amplitude from $x_I(t_I)$ to $x_F(t_F)$ is given by

$${}_H\langle x_F, t_F | x_I, t_I \rangle_H = {}_S\langle x_F | \hat{U}(t_F - t_I) | x_I \rangle_S, \quad (9)$$

where

$$\hat{U}(t) \equiv e^{-i\hat{H}t} \quad (10)$$

is a time-evolution operator. We now divide a time interval as follows

$$t_n \equiv t_I + n \cdot \epsilon, \quad (11)$$

where $n = 0, 1, \dots, N$. Therefore, we have a total of $N + 1$ points within the time interval, subject to the given conditions:

$$t_0 \equiv t_I; \quad t_N \equiv t_F; \quad t_F - t_I = N \cdot \epsilon. \quad (12)$$

We then find that the amplitude becomes

$$\begin{aligned} & {}_H\langle x_F, t_F | x_I, t_I \rangle_H \\ &= \lim_{N \rightarrow \infty} \int dx_1 dx_2 \cdots dx_{N-1} \\ & \quad \times {}_S\langle x_N | \hat{U}(\epsilon) | x_{N-1} \rangle_S {}_S\langle x_{N-1} | \hat{U}(\epsilon) | x_{N-2} \rangle_S \cdots {}_S\langle x_1 | \hat{U}(\epsilon) | x_0 \rangle_S. \end{aligned} \quad (13)$$

We now calculate the transition amplitude over a short time interval:

$$\begin{aligned} & {}_S\langle x_{n+1} | \hat{U}_L(\epsilon) | x_n \rangle_S \\ &= {}_S\langle x_{n+1} | 1 - i \cdot \epsilon \hat{H}_L(\hat{p}_n, \hat{x}_n) | x_n \rangle_S + \mathcal{O}(\epsilon^2) \\ &= \int dp_n {}_S\langle x_{n+1} | p_n \rangle_S {}_S\langle p_n | 1 - i \cdot \epsilon \hat{H}_L(\hat{p}_n, \hat{x}_n) | x_n \rangle_S + \mathcal{O}(\epsilon^2) \\ &= \frac{1}{\sqrt{2\pi}} \int dp_n e^{ip_n x_{n+1}} {}_S\langle p_n | 1 - i \cdot \epsilon \hat{H}_L(\hat{p}_n, \hat{x}_n) | x_n \rangle_S + \mathcal{O}(\epsilon^2) \\ &= \frac{1}{2\pi} \int dp_n e^{ip_n(x_{n+1} - x_n)} (1 - i \cdot \epsilon H_L(p_n, x_n)) + \mathcal{O}(\epsilon^2) \\ &= \int \frac{dp_n}{2\pi} \exp \left[i\epsilon \left(p_n \frac{x_{n+1} - x_n}{\epsilon} - H_L(p_n, x_n) \right) \right] + \mathcal{O}(\epsilon^2), \end{aligned} \quad (14)$$

where

$${}_S\langle p_j | x_k \rangle_S \equiv \frac{1}{\sqrt{2\pi}} e^{-ip_j x_k}. \quad (15)$$

Here, we add a subscript to the time-evolution operator to denote that the Hamiltonian is H_L . We can also derive the case for $\hat{U}_R(\epsilon)$ similarly. The result is

$$\begin{aligned} & {}_S\langle x_{n+1} | \hat{U}_R(\epsilon) | x_n \rangle_S \\ &= \int \frac{dp_n}{2\pi} \exp \left[i\epsilon \left(p_n \frac{x_{n+1} - x_n}{\epsilon} - H_R(p_n, x_{n+1}) \right) \right] + \mathcal{O}(\epsilon^2). \end{aligned} \quad (16)$$

When we meet the momentum operators, we insert a complete basis of momenta. Thus, the Hamiltonian is treated as a classical variable. This is the fundamental concept behind the derivation. Consequently, the Weyl ordering yields this result

$$\begin{aligned} & {}_S\langle x_{n+1} | \hat{U}_W(\epsilon) | x_n \rangle_S \\ &= \int \frac{dp_n}{2\pi} \exp \left[i\epsilon \left[p_n \frac{x_{n+1} - x_n}{\epsilon} - H_W \left(p_n, \frac{x_{n+1} + x_n}{2} \right) \right] \right] + \mathcal{O}(\epsilon^2). \end{aligned} \quad (17)$$

We drop the subscript in the time-evolution operator because we will always use Weyl ordering later

$$\begin{aligned} & {}_H\langle x_F, t_F | x_I, t_I \rangle_H \\ &= \lim_{N \rightarrow \infty} \int dx_1 dx_2 \cdots dx_{N-1} \frac{dp_0}{2\pi} \frac{dp_1}{2\pi} \cdots \frac{dp_{N-1}}{2\pi} \\ & \quad \times \exp \left[i \sum_{n=0}^{N-1} \epsilon \left[p_n \frac{x_{n+1} - x_n}{\epsilon} - H \left(p_n, \frac{x_{n+1} + x_n}{2} \right) \right] \right] + \mathcal{O}(\epsilon^2). \end{aligned} \quad (18)$$

We can formally write the amplitude as

$${}_H\langle x_F, t_F | x_I, t_I \rangle_H \equiv \int [dx dp] \exp \left(i \int_{t_I}^{t_F} dt (p\dot{x} - H(p, x)) \right). \quad (19)$$

The path integral formalism is just a phase space integral. The path integral formalism is useful because we only need to treat classical quantities using many properties of ordinary integrals. It is convenient for the goal of calculating.

It is clear from various orderings that different discretizations yield different results. Making different results makes sense because it encodes the information of the commutation relation between \hat{p} and \hat{x} . However, this makes the path integral more challenging than an ordinary integral

$$\lim_{N \rightarrow \infty} \sum_{n=0}^{N-1} \epsilon f(\xi_n) = \int_{t_I}^{t_F} dt f(t), \quad \xi_n \in [t_n, t_{n+1}]. \quad (20)$$

In an ordinary integral, any value of ξ_n within the interval $[t_n, t_{n+1}]$ can be used to obtain a result. However, this is different for the path integral. The primary reason for this difference is that the gap between x_{n+1} and x_n can be substantial even over a short time interval, as we consider all possible paths. An evaluation of the path integral is necessary on a finite lattice with a discretization scheme. The expression in a continuum limit is just formal for the convenience of writing due to the divergence. We consistently refer back to a discretized form whenever we perform a calculation.

Now, let us examine the simplest Hamiltonian

$$H(p, x) = \frac{p^2}{2} + V(x). \quad (21)$$

The transition amplitude becomes

$$\begin{aligned} & {}_H\langle x_F, t_F | x_I, t_I \rangle_H \\ &= \lim_{N \rightarrow \infty} \int dx_1 dx_2 \cdots dx_{N-1} \frac{dp_0}{2\pi} \frac{dp_1}{2\pi} \cdots \frac{dp_{N-1}}{2\pi} \\ & \quad \times \exp \left[i \sum_{n=0}^{N-1} \epsilon \left[p_n \frac{x_{n+1} - x_n}{\epsilon} - \frac{p_n^2}{2} - V \left(p_n, \frac{x_{n+1} + x_n}{2} \right) \right] \right] + \mathcal{O}(\epsilon^2). \end{aligned} \quad (22)$$

We can find that the integration of momenta is just a Gaussian integral:

$$\int_{-\infty}^{\infty} dx e^{-ax^2+bx+c} = \sqrt{\frac{\pi}{a}} e^{\frac{b^2}{4a}+c}; \quad \text{Re}(a) \geq 0, \quad a \neq 0. \quad (23)$$

Therefore, it is easy to evaluate. We conclude that:

$$\begin{aligned} & \int \frac{dp_n}{2\pi} \exp \left(-\frac{i\epsilon}{2} p_n^2 + i(x_{n+1} - x_n) p_n \right) = \frac{1}{\sqrt{2\pi i\epsilon}} \exp \left[\frac{i\epsilon}{2} \left(\frac{x_{n+1} - x_n}{\epsilon} \right)^2 \right]; \\ & {}_H\langle x_F, t_F | x_I, t_I \rangle_H \\ &= \lim_{N \rightarrow \infty} (2\pi i\epsilon)^{-\frac{N}{2}} \int dx_1 dx_2 \cdots dx_{N-1} \\ & \quad \times \exp \left[i \sum_{n=0}^{N-1} \epsilon \left[\frac{1}{2} \left(\frac{x_{n+1} - x_n}{\epsilon} \right)^2 - V \left(\frac{x_{n+1} + x_n}{2} \right) \right] \right] \\ &= \left(2\pi i \frac{t_F - t_I}{N} \right)^{-\frac{N}{2}} \int [dx] e^{i \int_{t_I}^{t_F} dt L(x, \dot{x})}, \end{aligned} \quad (24)$$

in which we use:

$$\epsilon = \frac{t_F - t_I}{N}; \quad \sum_{n=0}^{\infty} \epsilon \rightarrow \int_{t_I}^{t_F} dt; \quad \lim_{\epsilon \rightarrow 0} \frac{x_{n+1} - x_n}{\epsilon} \rightarrow \dot{x}. \quad (25)$$

Now, we obtain an integral path in a position space after integrating our momenta. Because the normalization factor does not depend on the positions, the factor can be ignored or canceled for normalization when one calculates correlation functions. However, the simple situation is not general after integrating out momenta. We will give an exact case to show such a situation when the potential depends on a velocity. However, the additional factor in the measure represents the quantum contribution to the action.

2.2 Non-Linear Theory

Now we consider the Lagrangian

$$L(x, \dot{x}) = \frac{1}{2} \dot{x}^2 f(x) - V(x), \quad (26)$$

which describes a system with a velocity-dependent potential. The function $f(x)$ is smooth. The momentum is:

$$p = \frac{\partial L}{\partial \dot{x}} = \dot{x} f(x). \quad (27)$$

Therefore, we derive the Hamiltonian:

$$H(p, x) = p\dot{x} - L = \frac{p^2}{f(x)} - \frac{p^2}{2f(x)} + V(x) = \frac{p^2}{2f(x)} + V(x). \quad (28)$$

The transition amplitude is:

$$\begin{aligned}
& {}_H \langle x_F, t_F | x_I, t_I \rangle_H \\
&= \lim_{N \rightarrow \infty} \int dx_1 dx_2 \cdots dx_{N-1} \frac{dp_0}{2\pi} \frac{dp_1}{2\pi} \cdots \frac{dp_{N-1}}{2\pi} \\
&\quad \times \exp \left[i \sum_{n=0}^{N-1} \epsilon \left[p_n \frac{x_{n+1} - x_n}{\epsilon} - \frac{p_n^2}{2f\left(\frac{x_{n+1} + x_n}{2}\right)} - V\left(\frac{x_{n+1} + x_n}{2}\right) \right] \right] + \mathcal{O}(\epsilon^2) \\
&= \lim_{N \rightarrow \infty} (2\pi i \epsilon)^{-\frac{N}{2}} \int dx_1 dx_2 \cdots dx_{N-1} \\
&\quad \times \exp \left[i \sum_{n=0}^{N-1} \epsilon \left[\frac{1}{2} \left(\frac{x_{n+1} - x_n}{\epsilon} \right)^2 f\left(\frac{x_{n+1} + x_n}{2}\right) - V\left(\frac{x_{n+1} + x_n}{2}\right) \right] \right] \\
&\quad \times \prod_{m=0}^{N-1} \sqrt{f\left(\frac{x_{m+1} + x_m}{2}\right)} \\
&= \lim_{N \rightarrow \infty} (2\pi i \epsilon)^{-\frac{N}{2}} \int dx_1 dx_2 \cdots dx_{N-1} \\
&\quad \times \exp \left[i \sum_{n=0}^{N-1} \epsilon \left[\frac{1}{2} \left(\frac{x_{n+1} - x_n}{\epsilon} \right)^2 f\left(\frac{x_{n+1} + x_n}{2}\right) - V\left(\frac{x_{n+1} + x_n}{2}\right) \right. \right. \\
&\quad \left. \left. - \frac{i}{2\epsilon} \ln f\left(\frac{x_{n+1} + x_n}{2}\right) \right] \right] \\
&= \left(2\pi i \frac{t_F - t_I}{N} \right)^{-\frac{N}{2}} \int [dx] \exp \left[i \int_{t_I}^{t_F} dt \left(L(x, \dot{x}) - \frac{i}{2\delta(0)} \ln f(x) \right) \right], \quad (29)
\end{aligned}$$

in which we use:

$$\epsilon = \frac{t_F - t_I}{N}; \quad \sum_{n=0}^{\infty} \epsilon \rightarrow \int_{t_I}^{t_F} dt; \quad \frac{1}{\epsilon} \delta_{jk} \rightarrow \delta(t_j - t_k); \quad \lim_{\epsilon \rightarrow 0} \frac{x_{n+1} - x_n}{\epsilon} \rightarrow \dot{x} \quad (30)$$

and one identity

$$\det A = e^{\text{Tr} \ln A}. \quad (31)$$

Thus, by integrating out momenta, we obtain the Lagrangian and gain an additional term from the measure.

2.3 Finite Temperature

The partition function at a finite temperature T is

$$Z_T = \text{Tr} \left(e^{-\beta H} \right), \quad (32)$$

where

$$\beta \equiv \frac{1}{T} \quad (33)$$

is the inverse temperature. We can identify β as *it*. In a 1D bosonic quantum field theory, the path integral at finite temperature is defined as follows

$$Z_T = \int [d\phi] \exp(-S_T(\phi)), \quad (34)$$

where

$$S_T(\phi) \equiv \int_0^\beta d\tau L_E(\phi). \quad (35)$$

The L_E is the Lagrangian for the Euclidean time. The scalar field satisfies the periodic boundary condition

$$\phi(\tau) = \phi(\tau + \beta). \quad (36)$$

If the Lagrangian for the scalar field theory is

$$L = -\frac{1}{2}\partial_t\phi\partial^t\phi - V(\phi), \quad (37)$$

the action at a finite temperature becomes

$$S_T(\phi) = \int_0^\beta d\tau \left(\frac{1}{2}(\partial_\tau\phi)^2 + V(\phi) \right). \quad (38)$$

In QFT at finite temperature, the process is equivalent to performing a Wick rotation, defined as $t \equiv -i\tau$. The path integral at finite temperature is similar to doing a path integral with finite time.

2.4 Measure

Now, we examine the issue of a measure in scalar field theory with a potential

$$V(\phi) = \frac{1}{2}m^2\phi^2 \quad (39)$$

at finite temperature. The scalar field satisfies the equation of motion

$$(-\partial_\tau^2 + m^2)\phi(\tau) = \lambda \cdot \phi(\tau). \quad (40)$$

We write $\phi(\tau)$ as

$$\phi(\tau) = \sum_n \phi_n \cdot f_n(\tau), \quad (41)$$

Because $\phi(\tau)$ is a real quantum field, the ϕ_n has the constraint

$$\phi_n^* = \phi_{-n}. \quad (42)$$

where n is an integer. Then the $f_n(\tau)$ can be

$$f_n(\tau) = \frac{1}{\sqrt{\beta}} \exp\left(\frac{2\pi i n \tau}{\beta}\right). \quad (43)$$

Therefore, we can determine the eigenvalue of $f_n(\tau)$

$$\lambda_n = m^2 + \frac{4\pi^2 n^2}{\beta^2}. \quad (44)$$

In other words, we solve the equation

$$(-\partial_\tau^2 + m^2)f_n(\tau) = \lambda_n \cdot f_n(\tau), \quad (45)$$

and the relation between the λ and λ_n is

$$\lambda = \sum_n \lambda_n. \quad (46)$$

The $f_n(\tau)$ satisfies the orthogonal condition

$$\int_0^\beta d\tau f_n(\tau)^* f_m(\tau) = \delta_{nm}. \quad (47)$$

The orthogonal condition implies

$$\phi_n = \int_0^\beta d\tau f_n^*(\tau) \phi(\tau). \quad (48)$$

The action, written in terms of modes, is

$$S_E = \frac{1}{2} \sum_n \lambda_n \phi_n^* \phi_n. \quad (49)$$

To normalize the partition function

$$Z_T = \int [d\phi] \exp(-S_E) = 1, \quad (50)$$

the measure $[d\phi]$ is defined as

$$[d\phi] \equiv \prod_n \left(\sqrt{\frac{\lambda_n}{\pi}} \cdot d\phi_n \right). \quad (51)$$

Hence we obtain

$$\langle e^{-r \cdot S_E} \rangle = \prod_n \left(\frac{1}{\sqrt{1+r}} \right) = 0, \quad (52)$$

where r is an arbitrary positive number. It is easy to know that the configuration with an infinite action vanishes. Therefore, this implies that the configuration with a finite action also vanishes. We only have two possibilities for such a situation. The first situation is no finite action. This situation is generally impossible because soliton solutions exist in QFT. Therefore, we anticipate a scenario in which a finite action has no measurable impact. The zero measure does not contribute to a path integral. Now, let us explore the partition function. The partition function is normalized, and all integration ranges extend from $-\infty$ to ∞ . We first define

$$\sqrt{\lambda_n} \phi_n \equiv a_n. \quad (53)$$

We can write the expression of the partition function as the following:

$$Z_T = \prod_n \lim_{L \rightarrow \infty} \int_{-L}^L \frac{da_n}{\sqrt{\pi}} e^{-\frac{1}{2}a_n^2} = 1. \quad (54)$$

If we change the ordering of the infinite limitation and infinite products, we obtain

$$\lim_{L \rightarrow \infty} \prod_n \int_{-L}^L \frac{da_n}{\sqrt{\pi}} e^{-\frac{1}{2}a_n^2} = \prod_n A_n(L) = 0, \quad (55)$$

where $A_n(L) < 1$. Before we take $L \rightarrow \infty$, the infinite products of $A_n(L)$ already vanish. Hence, we obtain the same conclusion. The configuration contributes to path integration only when the action becomes infinite (as $L \rightarrow \infty$). In other words, the finite action has zero measure.

Let us use the discretized version to revisit the issue

$$\frac{1}{2} \int dt \dot{\phi}^2 \rightarrow \frac{1}{2} \sum_j \frac{(\phi_{j+1} - \phi_j)^2}{\epsilon}. \quad (56)$$

The infinite action at least requires

$$\left\langle \frac{(\phi_{j+1} - \phi_j)^2}{\epsilon} \right\rangle \sim 1. \quad (57)$$

This results in a configuration that is not smooth

$$\dot{\phi}^2 \sim \frac{1}{\epsilon}. \quad (58)$$

The kinematic energy approaches infinity under the limit $\epsilon \rightarrow 0$. A configuration contributes to path integration only when it is not differentiable.

2.5 Perturbation Issue

The partition function of 0D QFT is just an integration:

$$Z(g) = \int_{-\infty}^{\infty} \frac{d\phi}{\sqrt{2\pi}} e^{-\frac{\phi^2}{2} - g\frac{\phi^4}{24}} = \sqrt{\frac{3}{2\pi g}} e^{\frac{3}{4g}} K_{\frac{1}{4}}\left(\frac{3}{4g}\right), \quad (59)$$

where $K_\nu(x)$ is the modified Bessel function of the second kind

$$K_\nu(z) \equiv \frac{\Gamma(\nu + \frac{1}{2})(2z)^\nu}{\sqrt{\pi}} \int_0^\infty dt \frac{\cos t}{(t^2 + z^2)^{\nu + \frac{1}{2}}}. \quad (60)$$

We can also use the weak-coupling perturbation to calculate the integration:

$$\begin{aligned} \frac{1}{\sqrt{2\pi}} \int_{-\infty}^{\infty} d\phi e^{-\frac{\phi^2}{2}} &= 1; \\ -g \frac{1}{4!\sqrt{2\pi}} \int_{-\infty}^{\infty} d\phi e^{-\frac{\phi^2}{2}} \phi^4 &= -\frac{g}{8}; \\ (-g)^2 \frac{1}{2!(4!)^2\sqrt{2\pi}} \int_{-\infty}^{\infty} d\phi e^{-\frac{\phi^2}{2}} \phi^8 &= \frac{35g^2}{384}; \\ (-g)^3 \frac{1}{3!(4!)^3\sqrt{2\pi}} \int_{-\infty}^{\infty} d\phi e^{-\frac{\phi^2}{2}} \phi^{12} &= -\frac{385g^3}{3072}; \\ (-g)^4 \frac{1}{4!(4!)^4\sqrt{2\pi}} \int_{-\infty}^{\infty} d\phi e^{-\frac{\phi^2}{2}} \phi^{16} &= \frac{25025g^4}{98304}; \\ (-g)^5 \frac{1}{5!(4!)^5\sqrt{2\pi}} \int_{-\infty}^{\infty} d\phi e^{-\frac{\phi^2}{2}} \phi^{20} &= -\frac{1616615g^5}{2359296}; \\ (-g)^6 \frac{1}{6!(4!)^6\sqrt{2\pi}} \int_{-\infty}^{\infty} d\phi e^{-\frac{\phi^2}{2}} \phi^{24} &= \frac{260275015g^6}{113246208}; \\ (-g)^7 \frac{1}{7!(4!)^7\sqrt{2\pi}} \int_{-\infty}^{\infty} d\phi e^{-\frac{\phi^2}{2}} \phi^{28} &= -\frac{929553625g^7}{100663296}; \end{aligned}$$

$$\ln Z(g) = -\frac{g}{8} + \frac{g^2}{12} - \frac{11g^3}{96} + \frac{17g^4}{72} - \frac{619g^5}{960} + \frac{709g^6}{324} - \frac{858437g^7}{96768} + \mathcal{O}(g^8). \quad (61)$$

Thus, the coefficient increases rapidly as the powers of g rise. Indeed, the perturbation series of the $\ln Z(g)$ is not convergent, and the coefficient of the g^m grows as $m!$. The series is only asymptotically convergent, meaning that including the first few terms at a small value of g produces an exact solution with good precision. Developing non-perturbative techniques to study a quantum system is essential because the weak-coupling perturbation expansion can be problematic not only in strong coupling regions but also in weak coupling regions due to the issue of non-convergence.

2.6 Fermion Fields

The fermion field is a Grassmann variable in a path formalism. The Grassmann variables satisfy the following algebra

$$\theta_j \theta_k = -\theta_k \theta_j. \quad (62)$$

Therefore, the algebra shows:

$$\theta_j^2 = -\theta_j^2 = 0 \quad (63)$$

for each j . This indicates that Grassmann variables cannot be considered numbers. Consider the below c -function

$$f(\eta) = a + \alpha\eta, \quad (64)$$

where a is a c -number, α is a Grassmann constant, and η is a Grassmann variable.

Now, we will discuss the integration of Grassmann variables. We first assume that the integration has some elementary properties:

$$\int d\eta (b_1 f(\eta) + b_2 g(\eta)) = b_1 \int d\eta f(\eta) + b_2 \int d\eta g(\eta); \quad \int d\eta \frac{\partial}{\partial \eta} f(\eta) = 0, \quad (65)$$

where b_1 and b_2 are c -constants. Requiring that the integration is translational invariance

$$\int d\eta f(\eta) = \int d\eta f(\eta + \beta), \quad (66)$$

where β is a Grassmann constant, we obtain:

$$a \int d\eta + \alpha \int d\eta \eta = \int d\eta (a + \alpha\eta + \alpha\beta) = (a + \alpha\beta) \int d\eta + \alpha \int d\eta \eta. \quad (67)$$

As a result, we derive additional rules for integration.:

$$\int d\eta = 0; \quad \int d\eta \eta = 1. \quad (68)$$

Now we consider the Grassmann variables and their complex conjugation, and we obtain

$$\int d\eta^* d\eta \exp(-\eta^* A \eta) = \det(A). \quad (69)$$

We show the calculation steps for the constant value for A :

$$\int d\eta^* d\eta \exp(-\eta^* A \eta) = \int d\eta^* d\eta (1 - \eta^* A \eta) = \int d\eta^* d\eta (1 + \eta \eta^* A) = A. \quad (70)$$

We find that integrating bosonic variables differs significantly from integrating Grassmann variables.

3 RG Flow

We introduce the concepts of RG flow [3] beginning from quantum mechanics (QM). We then discuss the relations between the physical, renormalized, and bare parameters in 4D $\lambda\phi^4$ theory. We present the Wilson and Polchinski exact renormalization group equation (ERGE) and discuss the triviality in 4D $\lambda\phi^4$ theory [32] from the Polchinski ERGE.

3.1 QM

The initial concept of RG flow indicates that parameters are influenced by regularization. The regularization is to modify a theory at a scale of a cut-off to a well-defined level. After the modification, the theory has been made more consistent and well-defined. We demonstrate the concept from QM

$$-\frac{1}{2}\nabla^2\Psi(x) + c \cdot \delta^2(x)\Psi(x) = E\Psi(x), \quad (71)$$

where E is the eigenenergy, the dimensionless parameter c does not depend on the spatial coordinates, and we solve the above equation from the spherically symmetric case Hence, the Hamiltonian becomes

$$-\frac{1}{2r} \frac{d}{dr} \left(r \frac{d\Psi}{dr} \right) + \frac{c}{2\pi r} \delta(r-a)\Psi(r) = E\Psi(r), \quad (72)$$

in which we used:

$$\nabla^2 \Psi = \frac{1}{r} \frac{d}{dr} \left(r \frac{d\Psi}{dr} \right); \quad \delta^2(x) \equiv \frac{1}{2\pi r} \delta(r) \rightarrow \frac{1}{2\pi r} \delta(r - a). \quad (73)$$

When $r \neq a$, the wavefunction is a linear combination of the Bessel function of the first kind $J_0(pr)$ and the Bessel function of the second kind $Y_0(pr)$. The Bessel functions for the integer n are defined as:

$$J_n(x) \equiv \frac{1}{\pi} \int_0^\pi d\tau \cos(n\tau - x \cdot \sin(\tau)); \quad Y_n(x) \equiv \lim_{\alpha \rightarrow n} \frac{J_\alpha(x) \cos(\alpha\pi) - J_{-\alpha}(x)}{\sin(\alpha\pi)}. \quad (74)$$

Therefore, the wavefunction is expressed as

$$\Psi(r) = \begin{cases} A \cdot J_0(pr) + B \cdot Y_0(pr) & r > a, \\ C \cdot J_0(pr), & r < a, \end{cases} \quad (75)$$

where

$$p = \sqrt{2E}. \quad (76)$$

Then, we multiply r by the equation

$$-\frac{1}{2} \frac{d}{dr} \left(r \frac{d\Psi}{dr} \right) + \frac{c}{2\pi} \delta(r - a) \Psi(r) = E \cdot r \Psi(r). \quad (77)$$

Then we integrate the equation for the r from $a - \epsilon$ to $a + \epsilon$ and take the limit $\epsilon \rightarrow 0$ in the final:

$$\begin{aligned} & \lim_{\epsilon \rightarrow 0} \int_{a-\epsilon}^{a+\epsilon} dr \left[-\frac{1}{2} \frac{d}{dr} \left(r \frac{d\Psi}{dr} \right) + \frac{c}{2\pi} \delta(r - a) \Psi(r) \right] \\ &= -\frac{a}{2} (\Psi'(a + \epsilon) - \Psi'(a - \epsilon)) + \frac{c}{2\pi} \Psi(a); \end{aligned}$$

$$E \lim_{\epsilon \rightarrow 0} \int_{a-\epsilon}^{a+\epsilon} dr r \Psi(r) = 0; \quad (78)$$

$$(79)$$

$$\Psi'(a + \epsilon) - \Psi'(a - \epsilon) = \frac{c}{\pi a} \Psi(a). \quad (80)$$

In this context, we assume that the wavefunction is continuous at $r = a$, but its derivative is not.

We now have two conditions: a continuous wavefunction and a discontinuous derivative to solve the equation of QM. When $r \gg a$, the wavefunction's asymptotic behavior is:

$$\Psi(r) \rightarrow A \cdot \cos\left(pr - \frac{\pi}{4}\right) + B \cdot \sin\left(pr - \frac{\pi}{4}\right) \propto \cos\left(pr - \frac{\pi}{4} + \delta_0\right), \quad (81)$$

where

$$\tan \delta_0 \equiv -\frac{A}{B}. \quad (82)$$

The coefficients A and B can be rewritten in terms of C :

$$\begin{aligned} A &= \left[1 - \frac{c}{\pi} \left[\ln\left(\frac{pa}{2}\right) + \gamma \right] + \mathcal{O}(p^2 a^2)\right] C; \\ B &= \left(\frac{c}{2} + \mathcal{O}(p^2 a^2)\right) C, \end{aligned} \quad (83)$$

where γ is the Euler-Mascheroni constant

$$\gamma = \lim_{n \rightarrow \infty} \left(-\ln n + \sum_{k=1}^n \frac{1}{k} \right), \quad (84)$$

for

$$p \ll \frac{1}{a}. \quad (85)$$

Hence we obtain

$$\cot \delta_0 = -\frac{2}{c} + \frac{2}{\pi} \left[\ln\left(\frac{pa}{2}\right) + \gamma \right] + \mathcal{O}(p^2 a^2). \quad (86)$$

It is easy to observe that the right-hand side depends on the regularization parameter a . However, the δ_0 is a physical observable. Therefore, the value of c must also depend on the value of a .

We now identify the regularization parameter as the momentum cutoff

$$a \equiv \frac{1}{\Lambda}. \quad (87)$$

Then we obtain:

$$\begin{aligned} 0 &= \frac{d}{d\Lambda} \cot \delta_0 = \left(\frac{\partial}{\partial \Lambda} + \frac{dc}{d\Lambda} \frac{\partial}{\partial c} \right) \cot \delta_0 \\ &= \frac{2}{\pi} \frac{2\Lambda}{p} \left(-\frac{p}{2\Lambda^2} \right) + \frac{dc}{d\Lambda} \frac{2}{c^2}, \end{aligned} \quad (88)$$

which leads to

$$\Lambda \frac{d}{d\Lambda} \left(\frac{1}{c} \right) = -\frac{1}{\pi}. \quad (89)$$

Therefore, the parameter is essential for the regularization process. The theoretical consistency requires that the regularization influence the parameter. Consequently, the RG flow is also necessary in QM. The parameter c is called the bare parameter. We also use an energy scale μ to define the renormalized parameter

$$\frac{1}{c_R(\mu)} \equiv \frac{1}{c(\Lambda)} - \frac{1}{\pi} \left[\ln \left(\frac{\mu}{2\Lambda} \right) + \gamma \right]. \quad (90)$$

A physical observable should not depend on the energy scale μ . Now we can rewrite the equation in terms of the renormalized parameter

$$\cot \delta_0 = -\frac{2}{c_R(\mu)} + \frac{2}{\pi} \ln \frac{p}{\mu} + \mathcal{O} \left(\frac{p^2}{\Lambda^2} \right). \quad (91)$$

Requiring that the δ_0 does not depend on the μ , and then it shows

$$\mu \frac{\partial}{\partial \mu} \left(\frac{1}{c_R} \right) = -\frac{1}{\pi}. \quad (92)$$

We are more interested in the renormalized parameter because it is closely related to the physical observable

$$\cot \delta_0 = -\frac{2}{c_R(\mu = p)} + \mathcal{O} \left(\frac{p^2}{\Lambda^2} \right). \quad (93)$$

The equation indicates that the momentum cut-off must exceed the energy scale. Otherwise, the running picture will become invalid. When the energy scale is reduced, maintaining the same low-energy physics requires adjusting the coupling constant.

3.2 4D $\lambda\phi^4$ Theory

We consider the 4D $\lambda\phi^4$ theory as an example. The Lagrangian is

$$L = -\frac{1}{2} \partial_\mu \phi \partial^\mu \phi - \frac{1}{2} (m^2 - i\epsilon) \phi^2 - \frac{\lambda}{4!} \phi^4. \quad (94)$$

Now, let us proceed to calculate the two-point function.

$$G_2(x, y) \equiv \langle \phi(x) \phi(y) \rangle. \quad (95)$$

We do an expansion up to the first-order in λ

$$G_2(x, y) = \frac{1}{Z[\lambda]} \int \mathcal{D}\phi e^{iS[\lambda=0]} \phi(x)\phi(y) \left[1 + \int d^4\tilde{x} \left(-i\frac{\lambda}{4!} \phi^4(\tilde{x}) \right) \right] + \dots, \quad (96)$$

where $Z[\lambda]$ is the partition function, and $S[\lambda]$ is the action. When one also expands the partition function in λ at the leading order, one can apply Wick's theorem to the calculation of correlation functions:

$$\begin{aligned} & \frac{1}{Z[\lambda=0]} \int \mathcal{D}\phi e^{iS[\lambda=0]} \phi(x)\phi(y) \left[1 + \int d^4\tilde{x} \left(-i\frac{\lambda}{4!} \phi^4(\tilde{x}) \right) \right] \\ = & \frac{1}{Z[\lambda=0]} \int \mathcal{D}\phi e^{iS[\lambda=0]} \phi(x)\phi(y) \\ & + \frac{1}{Z[\lambda=0]} \int \mathcal{D}\phi e^{iS[\lambda=0]} \phi(x)\phi(y) \int d^4\tilde{x} \left(-i\frac{\lambda}{4!} \phi^4(\tilde{x}) \right) \\ = & \tilde{G}_2(x, y) - \frac{i\lambda}{2} \int d^4\tilde{x} \tilde{G}_2(\tilde{x}, \tilde{x}) \tilde{G}_2(x, \tilde{x}) \tilde{G}_2(y, \tilde{x}) + \dots, \end{aligned} \quad (97)$$

where

$$\tilde{G}_2(x, y) \equiv i \int \frac{d^4p}{(2\pi)^4} \frac{e^{ip(x-y)}}{-p^2 - m^2 + i\epsilon}. \quad (98)$$

The \dots will be eliminated through the expansion of the partition function

$$-\frac{\lambda}{[Z[\lambda=0]]^2} \delta Z \int \mathcal{D}\phi e^{iS[\lambda=0]} \phi(x)\phi(y), \quad (99)$$

in which δZ is defined by:

$$Z[\lambda] \equiv Z[\lambda=0] + \lambda \cdot \delta Z + \dots; \quad \delta Z = \int \mathcal{D}\phi e^{iS[\lambda=0]} \int d^4\tilde{x} \left(\frac{-i}{4!} \phi^4(\tilde{x}) \right). \quad (100)$$

The integration in the momentum space is given by:

$$\begin{aligned}
& -\frac{i\lambda}{2} \int d^4\tilde{x} \tilde{G}_2(\tilde{x}, \tilde{x}) \tilde{G}_2(x, \tilde{x}) \tilde{G}_2(y, \tilde{x}) \\
= & -\frac{i\lambda}{2} \int d^4\tilde{x} \frac{d^4p_1}{(2\pi)^4} \frac{d^4p_2}{(2\pi)^4} \frac{d^4p_3}{(2\pi)^4} \\
& \times \frac{i}{-p_1^2 - m^2 + i\epsilon} \frac{i}{-p_2^2 - m^2 + i\epsilon} \frac{i}{-p_3^2 - m^2 + i\epsilon} e^{i(p_2x+p_3y)} e^{-i\tilde{x}(p_2+p_3)} \\
= & -\frac{i\lambda}{2} \int \frac{d^4p_1}{(2\pi)^4} \frac{d^4p_2}{(2\pi)^4} \frac{d^4p_3}{(2\pi)^4} \\
& \times \frac{i}{-p_1^2 - m^2 + i\epsilon} \frac{i}{-p_2^2 - m^2 + i\epsilon} \frac{i}{-p_3^2 - m^2 + i\epsilon} e^{i(p_2x+p_3y)} (2\pi)^4 \delta^4(p_2 + p_3) \\
= & -\frac{i\lambda}{2} \int \frac{d^4p_1}{(2\pi)^4} \frac{d^4p_2}{(2\pi)^4} \\
& \times \frac{i}{-p_1^2 - m^2 + i\epsilon} \frac{i}{-p_2^2 - m^2 + i\epsilon} \frac{i}{-p_3^2 - m^2 + i\epsilon} e^{ip_2(x-y)}. \tag{101}
\end{aligned}$$

Consequently, the two-point function in momentum space takes the following form

$$\bar{G}_2(p) = \frac{i}{-p^2 - m^2 + i\epsilon} - \frac{i\lambda}{2} \left(\frac{i}{-p^2 - m^2 + i\epsilon} \right)^2 \int \frac{d^4p_1}{(2\pi)^4} \frac{i}{-p_1^2 - m^2 + i\epsilon} + \dots \tag{102}$$

The quantum correction of the mass term is given by:

$$\begin{aligned}
\frac{i}{-p^2 - m^2 - \delta m^2 + i\epsilon} &= \frac{i}{(-p^2 - m^2 + i\epsilon) \left(1 - \frac{\delta m^2}{-p^2 - m^2 + i\epsilon}\right)} \\
&= \frac{i}{-p^2 - m^2 + i\epsilon} + \frac{i\delta m^2}{(-p^2 - m^2 + i\epsilon)^2} + \dots \tag{103}
\end{aligned}$$

Hence the δm^2 is

$$\delta m^2 = i\frac{\lambda}{2} \int \frac{d^4p}{(2\pi)^4} \frac{1}{-p^2 - m^2 + i\epsilon}. \tag{104}$$

Now we do a Wick rotation for the momentum

$$p^0 = ip_E^0. \tag{105}$$

The Euclidean metric is $\text{diag}(+, +, \dots, +)$. Then we obtain:

$$\begin{aligned}
\delta m^2 &= i\frac{\lambda}{2} \int \frac{d^4p}{(2\pi)^4} \frac{1}{-p^2 - m^2 + i\epsilon} = -\frac{\lambda}{2} \int \frac{d^4p_E}{(2\pi)^4} \frac{1}{-p_E^2 - m^2 + i\epsilon} \\
&= \frac{\lambda}{2} \int \frac{d^4p_E}{(2\pi)^4} \frac{1}{p_E^2 + m^2 - i\epsilon}. \tag{106}
\end{aligned}$$

We redefine the momentum as the below:

$$\begin{aligned}
p_{1,E} &\equiv p_E \sin(\theta_1) \sin(\theta_2) \cos(\phi); \\
p_{2,E} &\equiv p_E \sin(\theta_1) \sin(\theta_2) \sin(\phi); \\
p_{3,E} &\equiv p_E \sin(\theta_1) \cos(\theta_2); \\
p_{4,E} &\equiv p_E \cos(\theta_1).
\end{aligned} \tag{107}$$

The range of the variables is provided as follows:

$$0 \leq \theta_1 \leq \pi; \quad 0 \leq \theta_2 \leq \pi; \quad 0 \leq \theta_3 \leq 2\pi; \quad 0 \leq p_E \leq \Lambda. \tag{108}$$

Calculating the Jacobian matrix obtains:

$$\int d^4 p_{1,E} = \int_0^\pi d\theta_2 \sin^2(\theta_2) \int_0^\pi d\theta_1 \sin(\theta_1) \int_0^{2\pi} d\phi \int_0^\Lambda dp_E p_E^3 = 2\pi^2 \int_0^\Lambda dp_E p_E^3. \tag{109}$$

As a result, we can conclude the following:

$$\begin{aligned}
\delta m^2 &= \frac{\lambda}{2} \int \frac{d^4 p_{1,E}}{(2\pi)^4} \frac{1}{p_{1,E}^2 + m^2 - i\epsilon} = \frac{\lambda}{16\pi^2} \int_0^\Lambda dp_E p_E^3 \frac{1}{p_E^2 + m^2 - i\epsilon} \\
&= \frac{\lambda}{32\pi^2} \int_0^{\Lambda^2} du \frac{u}{u + m^2 - i\epsilon} = \frac{\lambda}{32\pi^2} \int_0^{\Lambda^2} du \left(1 - \frac{m^2 - i\epsilon}{u + m^2 - i\epsilon} \right) \\
&= \frac{\lambda}{32\pi^2} \left[\Lambda^2 - (m^2 - i\epsilon) \ln \left(1 + \frac{\Lambda^2}{m^2 - i\epsilon} \right) \right],
\end{aligned} \tag{110}$$

where

$$u \equiv p_E^2. \tag{111}$$

Indeed, we use the property of contour integration and assume some conditions. When the poles enclosed in the closed loops are the same, the value of the contour integration is not changed. We assume that the contour integral approaches zero at the boundary. We used the property and assumption to evaluate the above integration. The integration becomes divergent when the momentum approaches infinity. It is why we put a cut-off Λ in the momentum. The procedure is regularization. We will now discuss the assumptions related to the vanishing boundary integration. Indeed, the divergent boundary integration is not due to the time component of the momentum variable. More

precisely, the contour integration for the time component of the momentum variable without including the integration for the spatial components of the momentum variable has the vanishing boundary integration. To begin with, we perform a Wick rotation for the time component of the momentum variable and then proceed to integrate the spatial components of the momentum variable. Consequently, applying Wick's rotation only necessitates zero boundary integral of the time-component momentum variable.

Because the physical mass

$$m_{\text{phys}}^2 \equiv m^2 + \delta m^2 \quad (112)$$

is independent of the cut-off:

$$\frac{d}{d\Lambda} m_{\text{phys}}^2 = \frac{d}{d\Lambda} (m^2 + \delta m^2) = 0, \quad (113)$$

we obtain

$$\Lambda \frac{dm^2}{d\Lambda} = -\frac{\lambda}{16\pi^2} \left(\Lambda^2 - (m^2 - i\epsilon) \frac{\Lambda^2}{m^2 + \Lambda^2 - i\epsilon} \right) + \dots, \quad (114)$$

where \dots represents contributions from higher-order effects. Now, we will select a significantly high cutoff to achieve

$$\Lambda \frac{dm^2}{d\Lambda} \approx -\frac{\lambda}{16\pi^2} \left(\Lambda^2 - (m^2 - i\epsilon) \right) + \dots. \quad (115)$$

We can then solve the flow equation

$$m^2(\Lambda) \approx -\frac{\lambda}{32\pi^2} \left(\Lambda^2 - m^2 \ln \frac{\Lambda^2}{\mu^2} \right) + m_r^2, \quad (116)$$

in which the variables, energy scale μ and renormalized mass m_r , depend on the initial conditions of the flow equation, to obtain the bare mass:

$$m^2(\Lambda) \approx \frac{m_r^2 - \frac{\lambda}{32\pi^2} \Lambda^2}{1 - \frac{\lambda}{32\pi^2} \ln \frac{\Lambda^2}{\mu^2}} \approx m_r^2 \left(1 + \frac{\lambda}{32\pi^2} \ln \frac{\Lambda^2}{\mu^2} \right) - \frac{\lambda}{32\pi^2} \Lambda^2. \quad (117)$$

Therefore, the physical mass can be expressed as:

$$m_{\text{phys}}^2 = m^2 + \delta m^2 = m_r^2 \left(1 + \frac{\lambda}{32\pi^2} \ln \frac{m_r^2}{\mu^2} \right). \quad (118)$$

The physical mass is not affected by the momentum cut-off. When we choose $m_r^2 = \mu^2$, the square of physical mass is μ^2 again. Thus, we can see that the renormalized mass closely relates to the physical observable, which is the physical mass. The observation appeared in QM. We now utilize QFT to revisit this observation once more.

3.3 Wilson ERGE

The Wilson ERGE aims to create an adequate low-energy description by integrating a high-energy mode and maintaining the same partition function. We begin from a partition function with a momentum cut-off Λ and integrate out a high-energy mode:

$$\begin{aligned} Z &= \int_{p \leq \Lambda} \mathcal{D}\phi \exp(-S_\Lambda(\phi)) = \int_{p \leq \bar{\Lambda}} \mathcal{D}\phi_- \int_{\bar{\Lambda} \leq p \leq \Lambda} \mathcal{D}\phi_+ \exp(-S_\Lambda(\phi)) \\ &= \int_{p \leq \bar{\Lambda}} \mathcal{D}\phi_- \exp(-S_{\bar{\Lambda}}(\phi)), \end{aligned} \quad (119)$$

where

$$\exp(-S_{\bar{\Lambda}}(\phi)) \equiv \int_{\bar{\Lambda} \leq p \leq \Lambda} \mathcal{D}\phi_+ \exp(-S_\Lambda(\phi)). \quad (120)$$

We can determine that the operation is transitive. If we calculate $S_{\bar{\Lambda}}$ from the S_Λ and then calculate $S_{\bar{\bar{\Lambda}}}$ from the $S_{\bar{\Lambda}}$, it is equivalent to calculating $S_{\bar{\bar{\Lambda}}}$ from the S_Λ . Therefore, the transition indicates that the operation is associative

$$O_2 \circ (O_1 \circ S_\Lambda) = (O_2 \circ O_1) \circ S_\Lambda. \quad (121)$$

The $O_1 \circ S_\Lambda$ means the calculation of $S_{\bar{\Lambda}}$ from the S_Λ . The $O_2 \circ (O_1 \circ S_\Lambda)$ means the calculation of $S_{\bar{\bar{\Lambda}}}$ from the $S_{\bar{\Lambda}}$. The $(O_2 \circ O_1) \circ S_\Lambda$ means the calculation of $S_{\bar{\bar{\Lambda}}}$ from the S_Λ . Therefore, the Wilson ERGE is a semigroup. Because the operation for integrating out a high-energy mode does not have an inverse operation, Wilson ERGE is not a group. The Wilson ERGE offers a physical perspective for a theory with a cut-off, but its practical application is challenging. We will later introduce the Polchinski ERGE to simplify the calculations.

3.4 Polchinski ERGE

Now, we will illustrate how Polchinski discusses the ERGE in the context of scalar field theory. The Euclidean Lagrangian is

$$L_E = \frac{1}{2} \partial_\mu \phi \partial^\mu \phi + V(\phi) \equiv \frac{1}{2} \partial_\mu \phi \partial^\mu \phi + \sum_{k=1}^{\infty} \Lambda^{d-k(d-2)} \frac{\lambda_{2k}}{(2k!)} \phi^{2k}, \quad (122)$$

where d is the dimensions of spacetime. In this discussion, we focus on dimensionality greater than two, as operators involving derivatives, aside from the kinematic term, become irrelevant. The relevant operators characterize our macroscopic world. The

coupling constants λ_{2k} are dimensionless. We also require the symmetry $\phi \rightarrow -\phi$ in the Euclidean Lagrangian. Therefore, we can utilize the Euclidean Lagrangian to analyze Polchinski's ERGE in scalar field theory. We separate the scalar field from low- and high-energy modes as the following

$$\phi = \Phi + \chi. \quad (123)$$

Now we choose Φ as a constant background and then integrate out the high-energy mode χ . The quadratic effective action is given by

$$S_E[\Phi + \chi] - S_E[\Phi] = \int d^d x \left(\frac{1}{2} \partial_\mu \chi \partial^\mu \chi + \frac{1}{2} V''(\Phi) \chi^2 \right) + \dots, \quad (124)$$

in which \dots is the higher-order term of χ . After the Fourier transformation, the quadratic action becomes:

$$\begin{aligned} \int d^d x \left(\frac{1}{2} \partial_\mu \chi \partial^\mu \chi + \frac{1}{2} V''(\phi) \chi^2 \right) &= \int_{\Lambda - \delta\Lambda < |p| \leq \Lambda} \frac{d^d p}{(2\pi)^d} \bar{\chi}(p) \left(\frac{1}{2} p^2 + \frac{1}{2} V''(\Phi) \right) \bar{\chi}(-p) \\ &= \frac{\Lambda^{d-1} \delta\Lambda}{2(2\pi)^d} (\Lambda^2 + V''(\Phi)) \int_{S^{d-1}} d\Omega \bar{\chi}(\Lambda \hat{p}) \bar{\chi}(-\Lambda \hat{p}), \end{aligned} \quad (125)$$

where \hat{p} is a unit vector along the radial direction of a sphere. We select a small variation of the momentum cut-off. This facilitates the smooth integration of high-energy modes, simplifying the calculation of an RG flow. This is the main technique used in the Polchinski ERGE.

Now, we will integrate the high-energy mode to determine the variation of the cut-off in the effective action

$$e^{-\delta_\Lambda S_{\text{eff}}} \sim (\Lambda^2 + V''(\Phi))^{-\frac{N}{2}}, \quad (126)$$

where N is the number of momentum modes in the narrow shell. We do a regularization by placing the scalar field theory in a box with a size L and periodic boundary conditions. The momentum is quantized as follows

$$p_\mu \equiv \frac{2\pi}{L} n_\mu, \quad (127)$$

where n_ν is an arbitrary integer. Therefore, the number of momentum modes is given by

$$N = L^d \frac{\text{Vol}(S^{d-1})}{(2\pi)^d} \Lambda^{d-1} \delta\Lambda. \quad (128)$$

Hence we obtain

$$\delta_\Lambda S_{\text{eff}} = a\Lambda^{d-1}\delta\Lambda \int d^d x \ln(\Lambda^2 + V''(\Phi)), \quad (129)$$

where

$$a \equiv \frac{\text{Vol}(S^{d-1})}{2(2\pi)^d} = \frac{1}{(4\pi)^{\frac{d}{2}}\Gamma(\frac{d}{2})}, \quad (130)$$

and the integration comes from the factor L^d .

We combine the action and its correction and do the derivative for the momentum cut-off to obtain

$$\Lambda \frac{dS_{\text{eff}}}{d\Lambda} + \Lambda \frac{\delta_\Lambda S_{\text{eff}}}{\delta\Lambda} = 0, \quad (131)$$

which leads to the following:

$$\begin{aligned} &= \sum_{k=1}^{\infty} (d - (k(d-2)))\Lambda^{d-k(d-2)} \frac{\lambda_{2k}}{(2k)!} \Phi^{2k} \\ &\quad + \sum_{k=1}^{\infty} \Lambda^{d-k(d-2)} \frac{\Phi^{2k}}{(2k)!} \Lambda \frac{d\lambda_{2k}}{d\Lambda} \\ &\quad + a\Lambda^d \sum_{k=1}^{\infty} \left(\frac{1}{(2k)!} \frac{d^{2k}}{d\Phi^{2k}} \ln(\Lambda^2 + V''(\phi)) \right) \Big|_{\Phi=0} \Phi^{2k}; \end{aligned}$$

$$\Lambda \frac{d\lambda_{2k}}{d\Lambda} = (k(d-2) - d)\lambda_{2k} - a\Lambda^{k(d-2)} \frac{d^{2k}}{d\Phi^{2k}} \ln(\Lambda^2 + V''(\Phi)) \Big|_{\Phi} = 0. \quad (132)$$

The terms for $k=1$ and $k=2$ give:

$$\Lambda \frac{d\lambda_2}{d\Lambda} = -2\lambda_2 - a \frac{\lambda_4}{1+\lambda_2}; \quad \Lambda \frac{d\lambda_4}{d\Lambda} = (d-4)\lambda_4 - a \frac{\lambda_6}{1+\lambda_2} + 3a \frac{\lambda_4^2}{(1+\lambda_2)^2}. \quad (133)$$

We now assume that the coupling constants are weak, allowing us to linearize the flow equations as follows:

$$\beta_{2k} = \Lambda \frac{d\lambda_{2k}}{d\Lambda} = (k(d-2) - d)\lambda_{2k} - a\lambda_{2k+2}. \quad (134)$$

Hence we obtain a solution

$$\lambda_{2k} = 0 \quad (135)$$

for $k > 1$. This solution presents the most straightforward form of the fixed-point, known as the Gaussian fixed-point. We observe that the ϕ^2 term is relevant for $k = 1$ for a non-interacting theory. As soon as λ_2 becomes sufficiently large, the reliability of the approximation is compromised. Indeed, the exact solution shows that the β_{2k} approaches $(k(d-2) - d)\lambda_{2k}$ or the quantum correction is suppressed.

Now we consider $d = 4$, the coupling constants flow as the below:

$$\Lambda \frac{d\lambda_2}{d\Lambda} = -2\lambda_2 - a \frac{\lambda_4}{1 + \lambda_2}; \quad \Lambda \frac{d\lambda_4}{d\Lambda} = -a \frac{\lambda_6}{1 + \lambda_2} + 3a \frac{\lambda_4^2}{(1 + \lambda_2)^2}. \quad (136)$$

For the coupling constants $\lambda_6, \lambda_8, \dots$, etc., these represent irrelevant operators. Therefore, we can disregard these operators. The flow equations become:

$$\Lambda \frac{d\lambda_2}{d\Lambda} = -2\lambda_2 - a \frac{\lambda_4}{1 + \lambda_2}; \quad \Lambda \frac{d\lambda_4}{d\Lambda} \approx 3a \frac{\lambda_4^2}{(1 + \lambda_2)^2} = \frac{3}{16\pi^2} \lambda_4^2. \quad (137)$$

Therefore, the solution for λ_4 is as follows

$$\frac{1}{\lambda_4} = -\frac{3}{16\pi^2} \ln \Lambda + C_\Lambda, \quad (138)$$

where C_Λ is an arbitrary constant. We choose

$$C_\Lambda = \frac{3}{16\pi^2} \ln \mu \quad (139)$$

to obtain

$$\lambda_4(\Lambda) = \frac{16\pi^2}{3 \ln \left(\frac{\mu}{\Lambda} \right)}. \quad (140)$$

The ϕ^4 term is the highest power of ϕ in the relevant operators of 4D scalar field theory. For a consistent theory, it requires $\lambda_4 > 0$. Otherwise, the theory is not bounded when $|\phi| \rightarrow \infty$. This limits the available options

$$\mu > \Lambda. \quad (141)$$

Once we have obtained β_4 , we can determine the flow of the coupling constant. We need to worry about the divergence for the β_4 because it occurs at a finite scale $\Lambda = \mu$. This indicates that we do not have a non-trivial interacting QFT based on this result. To rely on the perturbation results in the 4D $\lambda\phi^4$ theory, we must select the cut-off scale and coupling constant to be as small as possible.

4 Lattice Formulations

We discuss the fermion doubling issue arising from naive lattice fermions and the more general Nielsen–Ninomiya no-go theorem [4, 5, 7]. The most common approach is to abandon (Wilson fermion [1]) or modify (overlap fermion [6]) the chiral symmetry. We present these approaches from the Wilson and overlap fermions. In particular, these two approaches are equivalent in the (1+1)D Hamiltonian formulation [12, 13, 14]. We then present a non-Hermitian lattice formulation that bypasses the no-go theorem by relaxing the requirement of Hermiticity [11].

4.1 Fermion Doubling

We introduce the doubling problem from the 1D Dirac fermion field. The Euclidean action is

$$S_D = \int dx \bar{\psi}(x)(\gamma_1 \partial_1 + m)\psi(x) \equiv \int dx \bar{\psi}(x)(D + m)\psi(x), \quad (142)$$

where

$$\gamma_1 \equiv \sigma_3 = \begin{pmatrix} 1 & 0 \\ 0 & -1 \end{pmatrix}; \quad \bar{\psi} \equiv \psi^\dagger \gamma_1; \quad \partial_1 \equiv \frac{\partial}{\partial x}. \quad (143)$$

The D is called the Dirac matrix. The propagator satisfies

$$\left(\gamma_1 \frac{d}{dx} + m \right) S(x) = \delta(x). \quad (144)$$

The solution is:

$$\begin{aligned} S(x) &= \int_{-\infty}^{\infty} \frac{dp}{2\pi} e^{ipx} \frac{1}{i\gamma_1 p + m} = \int_{-\infty}^{\infty} \frac{dp}{2\pi} e^{ipx} \frac{-i\gamma_1 p + m}{p^2 + m^2} \\ &= \left(-\gamma_1 \frac{d}{dx} + m \right) \int_{-\infty}^{\infty} \frac{dp}{2\pi} e^{ipx} \frac{1}{p^2 + m^2} = \left(-\gamma_1 \frac{d}{dx} + m \right) \frac{1}{2m} e^{-m|x|} \\ &= (\gamma_1 \cdot \text{sgn}(x) + 1) \frac{1}{2} e^{-m|x|} \\ &= \begin{pmatrix} \theta(x) & 0 \\ 0 & \theta(-x) \end{pmatrix} e^{-m|x|}, \end{aligned} \quad (145)$$

where

$$\theta(x) \equiv \begin{cases} 1, & x \geq 0 \\ 0, & x < 0 \end{cases}. \quad (146)$$

A naive discretization for the Euclidean action is:

$$\begin{aligned}
S_{DL} &= a \sum_{n=0}^{N-1} \bar{\psi}(n) \left(\gamma_1 \frac{\psi(n+1) - \psi(n-1)}{2a} + m\psi(n) \right) \\
&= a \sum_{n_1, n_2; \alpha_1, \alpha_2} \bar{\psi}(n_1)_{\alpha_1} (D(n_1, n_2)_{\alpha_1, \alpha_2} + m\delta_{\alpha_1, \alpha_2} \delta_{n_1, n_2}) \psi(n_2)_{\alpha_2}, \quad (147)
\end{aligned}$$

where

$$D(n_1, n_2)_{\alpha_1, \alpha_2} \equiv (\gamma_1)_{\alpha_1, \alpha_2} \frac{\delta_{n_1+1, n_2} - \delta_{n_1-1, n_2}}{2a}. \quad (148)$$

The matrix components of γ_1 are labeled by $\alpha_1, \alpha_2 = 1, 2$. The number of lattice points is given by N . The lattice fermion field satisfies the anti-periodic boundary condition

$$\psi(0) = -\psi(N). \quad (149)$$

Therefore, the propagator on the momentum space satisfies the following equations:

$$\left(\gamma_1 \frac{i \sin(pa)}{a} + m \right) \bar{S}(p) = 1; \quad \bar{S}(p) = \frac{1}{\gamma_1 \frac{i \sin(pa)}{a} + m}. \quad (150)$$

When the number of lattice points goes to infinity, the propagator in the position space becomes:

$$S_n = \int_{-\frac{\pi}{a}}^{\frac{\pi}{a}} \frac{dp}{2\pi} e^{ipna} \frac{1}{\gamma_1 \frac{i \sin(pa)}{a} + m} = \int_{-\frac{\pi}{a}}^{\frac{\pi}{a}} \frac{dp}{2\pi} e^{ipna} \begin{pmatrix} \frac{a}{i \sin(pa) + ma} & 0 \\ 0 & \frac{a}{-i \sin(pa) + ma} \end{pmatrix}. \quad (151)$$

After integrating the momentum, the first diagonal element is

$$S_{11}(x) = \begin{cases} \frac{(-ma + \sqrt{1+m^2a^2})^n}{\sqrt{1+m^2a^2}}, & x = na > 0 \\ (-1)^{|n|} \frac{(-ma + \sqrt{1+m^2a^2})^{|n|}}{\sqrt{1+m^2a^2}}, & x = na < 0 \end{cases}; \quad (152)$$

The second diagonal element is

$$S_{22}(x) = S_{11}(-x). \quad (153)$$

Now we take the continuum limit $ma \rightarrow 0$ with a fixed $x = na$ and then obtain

$$S_{11}(x) \rightarrow \begin{cases} e^{-m|x|}, & x > 0 \\ (-1)^{|n|} e^{-m|x|}, & x < 0 \end{cases}, \quad (154)$$

in which we used

$$\lim_{ma \rightarrow 0} \left(1 - ma\right)^{\frac{1}{ma}} = e. \quad (155)$$

It is easy to find that the propagator does not return to the expected continuum theory for $x < 0$. The reason is that we have two poles, which are at:

$$\gamma_1 \sin(pa) = ima; \quad \gamma_1 \sin(\pi - pa) = ima. \quad (156)$$

The appearance of the unwanted pole is due to the sine function. The non-perturbative effect of the lattice spacing non-trivially introduces the non-physical degrees to the fermion fields. In a continuum theory, we only have one pole in any dimension. When considering d dimensions, we have $2^d - 1$ unwanted poles.

The Nielsen-Ninomiya no-go theorem demonstrates that chiral symmetry and Fermion doubling cannot be simultaneously avoided when placing a Dirac fermion field on a lattice.[4, 5, 7]:

- 1. $D(x)$ is a local operator, which means it is bounded by $\sim \exp(-|x|/c)$, where c is proportional to the lattice spacing a ;
- 2. $\bar{D}(p) = i\gamma_\mu p_\mu + \mathcal{O}(ap^2)$ for $p \ll \pi/a$;
- 3. $\bar{D}(p)$ is invertible for $p \neq 0$ (no massless doublers);
- 4. $\gamma_5 D + D\gamma_5 = 0$ (chiral symmetry),

where the spacetime indices are denoted by μ . The common approach is to abandon or modify chiral symmetry on a lattice. The chiral transformation is

$$\psi \rightarrow e^{i\alpha\gamma_5} \psi; \quad \bar{\psi} \rightarrow \bar{\psi} e^{i\alpha\gamma_5}, \quad (157)$$

where α is a constant. The γ_5 satisfies the algebra

$$\gamma_\mu \gamma_5 + \gamma_5 \gamma_\mu = 0. \quad (158)$$

A chiral invariant Lagrangian must satisfy the following condition:

$$L_F = \bar{\psi} D \psi = \bar{\psi} e^{i\alpha\gamma_5} D e^{i\alpha\gamma_5} \psi. \quad (159)$$

This condition is equivalent to the condition

$$D\gamma_5 + \gamma_5 D = 0. \quad (160)$$

4.2 Wilson Fermion

To solve the doubling issue, we can introduce the Wilson term [1]

$$W_L = -a \frac{\delta_{a_1, a_2} \delta_{n_1+1, n_2} - 2\delta_{a_1, a_2} \delta_{n_1, n_2} + \delta_{a_1, a_2} \delta_{n_1-1, n_2}}{2a^2} \quad (161)$$

to generate an infinite mass for the unwanted pole at the continuum limit [1]. The Wilson term at a continuum limit is

$$W_L \sim -\frac{a}{2} \partial_1 \partial_1. \quad (162)$$

Because the kinematic term only has one derivative, it is easy to know that a higher derivative term should vanish at a continuum limit. The propagator is [1]

$$S_{DL} = \int_{-\frac{\pi}{a}}^{\frac{\pi}{a}} \frac{dp}{2\pi} e^{ipna} \frac{1}{\gamma_1 \frac{i \sin(pa)}{a} + m + \frac{1}{a} (1 - \cos(pa))}. \quad (163)$$

Therefore, we can determine that the mass of the unwanted pole is given by the expression $m + 2/a$ [1]. This mass becomes infinitely heavy in the continuum limit. When we take the continuum limit, the unwanted pole becomes irrelevant. However, the massless fermion makes reaching an expected continuum theory hard, and the Wilson fermion does not preserve chiral symmetry in a finite lattice [1].

4.3 Overlap Fermion

We first introduce the lattice chiral symmetry [9] given by the Ginsparg-Wilson relation [8]. We then discuss the spectrum of the Dirac operator satisfying the Ginsparg-Wilson relation. Ultimately, we offer a solution, the overlap fermion.

4.3.1 Lattice Chiral Symmetry

Indeed, the lattice artifact can modify the symmetry of a lattice. Hence, modifying the chiral transformation on a finite lattice is fine. We adopt the chiral transformation [9]:

$$\psi \rightarrow \exp \left[i\alpha \gamma_5 \left(1 - \frac{a}{2} D \right) \right] \psi; \quad \bar{\psi} \rightarrow \bar{\psi} \exp \left[i\alpha \left(1 - \frac{a}{2} D \right) \gamma_5 \right]. \quad (164)$$

When the fermion field interacts with other fields, the chiral transformation on a lattice can depend on the fields. The continuum transformation does not depend on fields due to the coupling. Hence, the chiral symmetry of a lattice fermion field is different from that of the continuum case.

Due to the chiral transformation, the chiral invariant Lagrangian requires the condition

$$\bar{\psi}D\psi = \bar{\psi} \exp \left[i\alpha \left(1 - \frac{a}{2}D \right) \gamma_5 \right] D \exp \left[i\alpha \gamma_5 \left(1 - \frac{a}{2}D \right) \right] \psi. \quad (165)$$

The above equality can be held:

$$\begin{aligned} & \bar{\psi} \exp \left[i\alpha \left(1 - \frac{a}{2}D \right) \gamma_5 \right] D \exp \left[i\alpha \gamma_5 \left(1 - \frac{a}{2}D \right) \right] \psi \\ &= \bar{\psi} \exp \left[i\alpha \left(1 - \frac{a}{2}D \right) \gamma_5 \right] \exp \left[-i\alpha \left(1 - \frac{a}{2}D \right) \gamma_5 \right] D\psi \\ &= \bar{\psi}D\psi \end{aligned} \quad (166)$$

when D satisfies

$$D\gamma_5 \left(1 - \frac{a}{2}D \right) + \left(1 - \frac{a}{2}D \right) \gamma_5 D = 0, \quad (167)$$

which is equivalent to the Ginsparg-Wilson relation [8]

$$D\gamma_5 + \gamma_5 D = aD\gamma_5 D. \quad (168)$$

4.3.2 Spectrum of Dirac Operator

Now, we will discuss the eigenvalues of the Dirac operator

$$Dv_\lambda = \lambda v_\lambda, \quad (169)$$

when the operator satisfies the Ginsparg-Wilson relation. The Dirac operator is γ_5 -Hermitian

$$\gamma_5 D \gamma_5 = D^\dagger, \quad (170)$$

which leads to the following:

$$\begin{aligned} \det(D - \lambda) &= \det(\gamma_5^2(D - \lambda)) = \det(\gamma_5(D - \lambda)\gamma_5) \\ &= \det(D^\dagger - \lambda) = (\det(D - \lambda^*))^*. \end{aligned} \quad (171)$$

The findings suggest that the eigenvalues are either real numbers or occur in pairs of complex conjugates:

$$\lambda(v_\lambda, \gamma_5 v_\lambda) = (v_\lambda, \gamma_5 D v_\lambda) = (v_\lambda, D^\dagger \gamma_5 v_\lambda) = (D v_\lambda, \gamma_5 v_\lambda) = \lambda^*(v_\lambda, \gamma_5 v_\lambda), \quad (172)$$

in which the inner product of two vectors, u_1 and u_2 , are defined by

$$(u_1, u_2) \equiv u_1^\dagger u_2. \quad (173)$$

Hence, this directly implies

$$(v_\lambda, \gamma_5 v_\lambda) = 0 \quad (174)$$

when λ is not real-valued. In other words, we have the non-vanishing chirality

$$(v_\lambda, \gamma_5 v_\lambda) \neq 0 \quad (175)$$

for real eigenvalues.

The Ginsparg-Wilson relation implies that D is a normal operator:

$$DD^\dagger = D^\dagger D = D + D^\dagger. \quad (176)$$

The eigenvectors form an orthogonal basis. The eigenvalues follow the equation

$$\lambda^* + \lambda = a\lambda^*\lambda. \quad (177)$$

When the definition of an eigenvalue is as follows

$$\lambda = x + iy, \quad (178)$$

we can obtain the Ginsparg-Wilson circle (Fig. 1)

$$\left(x - \frac{1}{a}\right)^2 + y^2 = \frac{1}{a^2}. \quad (179)$$

It is easy to know that we have two real eigenvalues:

$$0; \frac{2}{a}. \quad (180)$$

The unwanted mode, $2/a$, will decouple from the continuum limit.

When the eigenvector corresponds to a zero mode, we obtain the following:

$$Dv_0 = 0 \rightarrow 0 = \gamma_5 Dv_0 = (aD\gamma_5 D - D\gamma_5)v_0 = -D\gamma_5 v_0. \quad (181)$$

Since the Dirac operator acting on the zero-mode eigenvector commutes with γ_5 , one can select zero modes as the eigenstates of γ_5 . Since

$$\gamma_5^2 = 1, \quad (182)$$

we obtain

$$\gamma_5 v_0 = \pm v_0. \quad (183)$$

This indicates that the zero modes exhibit chirality. The right-handed mode has the positive chirality, and the left-handed mode has the negative chirality.

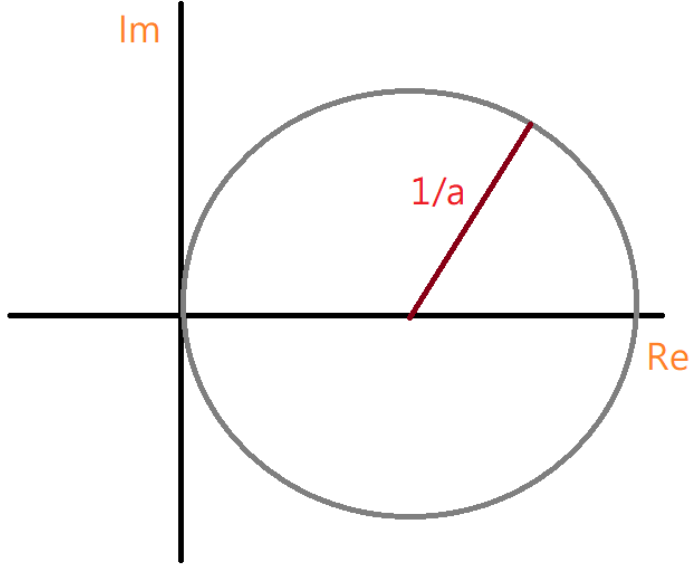


Figure 1: The real and imaginary parts of the eigenvalues lie on a circle centered at $x = \frac{1}{a}$, $y = 0$, with a radius of $1/a$.

4.3.3 Overlap Dirac Operator

Now we show one solution, overlap Dirac operator [6] to the Ginsparg-Wilson relation:

$$D_{ov} = \frac{1}{a}(1 + \gamma_5 \text{sgn}(Q)) = \frac{1}{a} \left(1 + \gamma_5 Q(Q^2)^{-\frac{1}{2}} \right); \quad Q = \gamma_5 A, \quad (184)$$

where A is some suitable operator with the γ_5 -Hermitian. Because the operator A satisfies the γ_5 -Hermitian, this shows that Q is Hermitian, which implies only real eigenvalues,

$$Q^\dagger = A^\dagger \gamma_5 = \gamma_5 A \gamma_5 \gamma_5 = \gamma_5 A = Q. \quad (185)$$

One choice for A is [6]

$$A = aD_W - (1 + s), \quad (186)$$

where D_W is the Wilson-Dirac operator, and $|s|$ is bounded by one

$$|s| < 1. \quad (187)$$

The overlap Dirac operator becomes [6]:

$$D_{ov} = \frac{1}{a} \left(1 + A(\gamma_5 A \gamma_5 A)^{-\frac{1}{2}} \right) = \frac{1}{a} \left(1 + A(A^\dagger A)^{-\frac{1}{2}} \right). \quad (188)$$

Therefore, we can show that [6]:

$$\begin{aligned} aD_{ov}D_{ov}^\dagger &= \frac{1}{a}(1 + \gamma_5 \text{sign}(Q))(1 + \text{sign}(Q)\gamma_5) = \frac{1}{a}(1 + \gamma_5 \text{sign}(Q) + \text{sign}(Q)\gamma_5 + 1) \\ &= D_{ov} + D_{ov}^\dagger. \end{aligned} \quad (189)$$

The overlap construction transforms the non-chiral Dirac operator D_W to a solution satisfying the Ginsparg-Wilson relation for establishing the lattice chiral symmetry.

4.4 (1+1)D Hamiltonian Formulation

When considering the (1+1)D Hamiltonian, we only have one spatial direction on the Wilson-Dirac operator. Therefore, one can show [14]

$$A^\dagger(s=0)A(s=0) = 1. \quad (190)$$

Hence, it implies that the overlap operator is the same as the Wilson-Dirac operator for a particular choice of s [14], $s = 0$,

$$D_{ov}(s=0) = \frac{1}{a}(1 + A(s=0)) = D_W. \quad (191)$$

This result is exciting because it implies that the Wilson fermion also has the lattice chiral symmetry as in the overlap fermion. Because the Wilson term generates the unwanted pole to the propagator, it implies that the lattice chiral symmetry allows non-zero physical mass on a finite lattice.

4.5 Non-Hermitian Lattice Formulation

The most straightforward method of realizing the non-Hermitian lattice formulation is to adopt the one-sided lattice differences [11]. The lattice action adopting the forward finite-difference is [11]:

$$\begin{aligned} S_{F1} &= a \sum_{n=0}^{N-1} \bar{\psi}(n) \left(\gamma_1 \frac{\psi(n+1) - \psi(n)}{a} + m\psi(n) \right) \\ &= a \sum_{n_1, n_2; \alpha_1, \alpha_2} \bar{\psi}(n_1)_{\alpha_1} (D(n_1, n_2)_{\alpha_1, \alpha_2} + m\delta_{n_1, n_2} \delta_{\alpha_1, \alpha_2}) \psi(n_2)_{\alpha_2}, \end{aligned} \quad (192)$$

where

$$D(n_1, n_2)_{\alpha_1, \alpha_2} \equiv (\gamma_1)_{\alpha_1, \alpha_2} \frac{\delta_{n_1+1, n_2} - \delta_{n_1, n_2}}{a}. \quad (193)$$

The lattice propagator in the infinite size limit is [27]:

$$\begin{aligned} S_{11}(x) &\rightarrow \begin{cases} (1 - ma)^{n-1}, & x > 0 \\ 0, & x < 0 \end{cases}; \\ S_{22}(x) &\rightarrow \begin{cases} 0, & x > 0 \\ (1 + ma)^{n-1}, & x < 0 \end{cases}. \end{aligned} \quad (194)$$

The continuum limit ($ma, a/x \rightarrow 0$) shows the exact propagator as in the free Dirac fermion theory [27]. We only have one pole in the continuum limit [27]. Because we replace $i \sin(pa)$ with $\exp(ipa)$, the number of poles reduces by half compared to the naive fermion.

When $d > 1$, the non-physical poles appear, but these poles do not provide the additional degrees of freedom when taking the continuum limit [11]. We aim to demonstrate such a result from the 2D case. When considering the non-Hermitian lattice formulation, the Dirac matrix is represented as follows [11]:

$$\bar{D}(p) = \frac{1}{a} \sum_{\mu=1}^4 \gamma_{\mu} (\exp(ip_{\mu}a) - 1) = \frac{2i}{a} \sum_{\mu=1}^2 \gamma_{\mu} e^{i\frac{p_{\mu}a}{2}} \sin\left(\frac{p_{\mu}a}{2}\right). \quad (195)$$

The inverse Dirac matrix is [11]:

$$\bar{D}^{-1}(p) = \frac{-\frac{i}{2a} \sum_{\mu=1}^2 \gamma_{\mu} e^{i\frac{p_{\mu}a}{2}} \sin\left(\frac{p_{\mu}a}{2}\right)}{\frac{1}{a^2} \sum_{\nu=1}^2 e^{ip_{\nu}a} \sin^2\left(\frac{p_{\nu}a}{2}\right)}. \quad (196)$$

It is straightforward to find the following non-physical poles:

$$p_1 a = -p_2 a = \pm \frac{\pi}{2}. \quad (197)$$

However, the expansion of $\exp(ip_{\mu}a) \sin^2(p_{\mu}a/2)/a^2$ around these non-physical poles does not shift the mass pole because there is no quadratic term [11]. When the non-physical poles shift mass, the mass becomes infinite in the continuum limit [11]. Generalizing to the general d -dimension can also evade the fermion doubling [11].

The one-sided lattice difference breaks the hypercubic symmetry [11]. In general, loss of the hypercubic symmetry implies non-renormalizability [11]. We need to consider the quenched averaging, which imposes the hypercubic symmetry at the observable level [11]

$$\overline{\langle \mathcal{O} \rangle} \equiv \frac{1}{2^d} \sum_{\epsilon_{\mu}=\pm 1} \langle \mathcal{O}(\epsilon_{\mu}) \rangle_{\epsilon_{\mu}}. \quad (198)$$

5 Numerical Algorithms

We introduce the MC method: Metropolis and Hybrid Monte Carlo (HMC). The HMC is the most efficient method for simulating the lattice field theory. Since the lattice fermion field is represented as a Grassmann variable, we aim to improve the naive implementation of the Monte Carlo method by substituting the fermion field with a pseudo-fermion field (a bosonic field). We also introduce the necessary numerical algorithms for generating random numbers following the Gaussian distribution and solving the linear equations. Because the non-Hermitian lattice formulation loses the Hermiticity in the Lagrangian, we cannot naively apply the MC simulation to the lattice system. This issue can be avoided when the partition function is non-negative [27].

5.1 MC Method

We first introduce the basic idea of the MC method. We then see how this method reaches the equilibrium through the detailed balance. The numerical algorithm of the MC method is based on the principles introduced by Metropolis and HMC.

5.1.1 Basic Idea

Systems with a significant physical degree of freedom are interesting in physics. To investigate such systems, one should involve an evaluation of higher-dimensional integration. The exact solution for the integral is generally unknown. A straightforward numerical study like the Runge-Kutta method is also impossible. When considering N atoms at a finite temperature T , the integration must be evaluated at 10^{3N} points if each site takes ten different values. Hence, it is impossible to do a large N study. The main idea of the MC simulation is not to evaluate the integrand at each point but to sample a point with the Boltzmann distribution in the integrand. The MC method can estimate a multiple integral better than a direct numerical study.

Consider the integral

$$I = \int_0^1 dx f(x). \quad (199)$$

Choosing N points randomly (with equal probability) in the interval $[0, 1]$,

$$I \approx \frac{1}{N} \sum_{j=1}^N f(x_j). \quad (200)$$

This method is known as simple sampling.

Now introduce a weight function $w(x)$ satisfying

$$\int_0^1 dx w(x) = 1. \quad (201)$$

The integral can be expressed in the following way:

$$I = \int_0^1 dx w(x) \frac{f(x)}{w(x)} = \int_0^1 dy \frac{f(x(y))}{w(x(y))} = \int_0^1 dy F(y), \quad (202)$$

where

$$y(x) \equiv \int_0^x dt w(t). \quad (203)$$

Sampling y uniformly is equivalent to sampling x using the weight function $w(x)$. Choosing more sampling at locations with a larger f is more effective. This technique is known as importance sampling. It is also the main idea of the MC simulation.

Now, we give an example to show the weight function. We choose that:

$$\begin{aligned} f(x) &= \frac{1}{1+x^2}; & I &= \int_0^1 dx f(x); \\ w(x) &= \frac{4-2x}{3}; & y &= \int_0^x dx w(x) = \frac{x(4-x)}{3}; \\ & & x &= 2 - \sqrt{4-3y}. \end{aligned} \quad (204)$$

However, it is hard to find such a weight function in general. Hence, we will introduce some algorithms for a more general study.

5.1.2 Detailed Balance

The detailed balance is

$$\frac{P(\vec{y} \rightarrow \vec{x})}{P(\vec{x} \rightarrow \vec{y})} = \frac{w(\vec{x})}{w(\vec{y})}, \quad (205)$$

in which the $P(\vec{x} \rightarrow \vec{y})$ is the probability of transition from the \vec{x} to the \vec{y} . The transition probability can be expressed as the product of the trial step probability from \vec{x} to \vec{y} , denoted as $T(\vec{x} \rightarrow \vec{y})$, and the acceptance probability of that step, $A(\vec{x} \rightarrow \vec{y})$

$$P(\vec{x} \rightarrow \vec{y}) = T(\vec{x} \rightarrow \vec{y}) \cdot A(\vec{x} \rightarrow \vec{y}). \quad (206)$$

Later, we will show that each algorithms have a probability distribution of $w(\vec{x})$ when a system goes to equilibrium.

5.1.3 Metropolis

The Metropolis algorithm is a general scheme for producing random variables with a given probability distribution of an arbitrary form. It only requires calculating a weight function at each step of updating. We first introduce the algorithm and then show the detailed balance for the algorithm. The algorithm of Metropolis for a system is:

- (a) The new configuration σ'_j is selected with an arbitrary probability distribution satisfying

$$T(\sigma_j \rightarrow \sigma'_j) = T(\sigma'_j \rightarrow \sigma_j). \quad (207)$$

- (b) Compute the change in energy

$$\Delta E = E(\sigma'_j) - E(\sigma_j). \quad (208)$$

- (c) If

$$\Delta E \leq 0, \quad (209)$$

the new configuration σ'_j is accepted, otherwise generate a random number $r \in (0, 1)$ with uniform deviate. If

$$r \leq \exp(-\beta\Delta E), \quad (210)$$

the new configuration is accepted. This provides the

$$A(\sigma_j \rightarrow \sigma'_j) = \min \left(1, \frac{\exp(-\beta E(\sigma'_j))}{\exp(-\beta E(\sigma_j))} \right). \quad (211)$$

- (d) Repeat the same procedure for another configuration.

The main limitation of the Metropolis algorithm is that the likelihood of accepting a new configuration is relatively low unless the new one closely resembles an old one. This drawback leads to a strongly correlated configuration with a long correlation time, which creates a serious problem at a phase transition point. This phenomenon is known as a critical slowdown.

In the Metropolis algorithm, it satisfies:

$$T(\vec{x} \rightarrow \vec{y}) = T(\vec{y} \rightarrow \vec{x}); \quad A(\vec{x} \rightarrow \vec{y}) = \min \left(1, \frac{w(\vec{y})}{w(\vec{x})} \right). \quad (212)$$

At the equilibrium, the net number of points moving from the \vec{x} to another point \vec{y} in the next step is:

$$\delta\rho(\vec{x}) = \rho_n(\vec{x})P(\vec{x} \rightarrow \vec{y}) - \rho_n(\vec{y})P(\vec{y} \rightarrow \vec{x}) = 0, \quad (213)$$

where $\rho_n(\vec{x})$ is the density of points at \vec{x} after n steps. Hence, we obtain the detailed balance as follows:

$$\frac{\rho_n(\vec{x})}{\rho_n(\vec{y})} = \frac{P(\vec{y} \rightarrow \vec{x})}{P(\vec{x} \rightarrow \vec{y})} = \frac{T(\vec{y} \rightarrow \vec{x})A(\vec{y} \rightarrow \vec{x})}{T(\vec{x} \rightarrow \vec{y})A(\vec{x} \rightarrow \vec{y})} = \frac{A(\vec{y} \rightarrow \vec{x})}{A(\vec{x} \rightarrow \vec{y})} = \frac{\min\left(1, \frac{w(\vec{x})}{w(\vec{y})}\right)}{\min\left(1, \frac{w(\vec{y})}{w(\vec{x})}\right)} = \frac{w(\vec{x})}{w(\vec{y})}. \quad (214)$$

5.1.4 HMC

To improve the drawback of Metropolis, we need an algorithm with the following properties:

- (i) efficient computation;
- (ii) acceptance probability is high even for a large lattice;
- (iii) weak correlation between successive configurations.

The HMC is an algorithm for updating all fields simultaneously with a high enough probability of accepting efficiently. Consider a field theory with the action $S(\phi)$, where ϕ denotes a generic field variable:

- 1. Initial configuration ϕ .
- 2. Generate momenta π with Gaussian distribution

$$P_G(\pi) \propto \exp(-\pi^2/2). \quad (215)$$

- 3. Molecular dynamics step (time length=1):

$$\dot{\phi} = \frac{\partial H}{\partial \pi}, \quad \dot{\pi} = -\frac{\partial H}{\partial \phi} = -\frac{\partial S}{\partial \phi}, \quad H(\phi, \pi) = \frac{\pi^2}{2} + S(\phi). \quad (216)$$

- 4. $P_A(\{\phi, \pi\} \rightarrow \{\phi', \pi'\}) = \min(1, \exp(-\Delta H))$, where

$$\Delta H = H(\phi', \pi') - H(\phi, \pi). \quad (217)$$

- 5. Go to 2.

The leap-frog algorithm for molecular dynamics (Molecular dynamics step) is:

- 1. Initial half-step for the π :

$$\phi(0) = \phi; \quad \pi\left(\frac{\epsilon}{2}\right) = \pi(0) - \frac{\epsilon}{2} \frac{\partial S(\phi)}{\partial \phi(0)}, \quad (218)$$

where ϵ is the discrete time step.

- 2. Intermediate $N - 1$ steps ($\tau = n\epsilon, n = 1, 2, \dots, N - 1$):

$$\begin{aligned} \phi(\tau) &= \phi(\tau - \epsilon) + \epsilon \cdot \pi\left(\tau - \frac{\epsilon}{2}\right); \\ \pi\left(\tau + \frac{\epsilon}{2}\right) &= \pi\left(\tau - \frac{\epsilon}{2}\right) - \epsilon \frac{\partial S(\phi)}{\partial \phi(\tau)}. \end{aligned} \quad (219)$$

- 3. Final step for the ϕ (half-step for the π):

$$\begin{aligned} \phi' &= \phi(1) = \phi(1 - \epsilon) + \epsilon \cdot \pi\left(1 - \frac{\epsilon}{2}\right); \\ \pi' &= \pi(1) = \pi\left(1 - \frac{\epsilon}{2}\right) - \frac{\epsilon}{2} \frac{\partial S(\phi)}{\partial \phi(1)}. \end{aligned} \quad (220)$$

The leap-frog algorithm has the reversibility

$$\{\phi', -\pi'\} \rightarrow \{\phi, -\pi\}. \quad (221)$$

The detailed balance is demonstrated as follows:

- 1. $P_G = c \cdot \exp(-\pi^2/2)$ and $\int d\pi P_G(\pi) = 1$.
- 2. Reversibility is the molecular dynamics:

$$\begin{aligned} \{\phi, \pi\} \rightarrow \{\phi', \pi'\} &\Rightarrow \{\phi', -\pi'\} \rightarrow \{\phi, -\pi\}; \\ P_M(\{\phi, \pi\} \rightarrow \{\phi', \pi'\}) &= P_M(\{\phi', -\pi'\} \rightarrow \{\phi, -\pi\}). \end{aligned} \quad (222)$$

- 3. The Metropolis test

$$P_A(\{\phi, \pi\} \rightarrow \{\phi', \pi'\}) = \min(1, \exp(-\Delta H)), \quad (223)$$

where

$$\Delta H = H(\phi', \pi') - H(\phi, \pi); \quad H(\phi, \pi) = \frac{\pi^2}{2} + S(\phi). \quad (224)$$

Then we have:

$$\begin{aligned}
P(\phi \rightarrow \phi') &= \int d\pi d\pi' P_G(\pi) P_M(\{\phi, \pi\} \rightarrow \{\phi', \pi'\}) P_A(\{\phi, \pi\} \rightarrow \{\phi', \pi'\}), \\
P_{\text{eq}}(\phi) &\propto e^{-S(\phi)}, \\
\int d\phi P_{\text{eq}}(\phi) &= 1.
\end{aligned} \tag{225}$$

- Finally, we show that:

$$\begin{aligned}
&P_{\text{eq}}(\phi) P(\phi \rightarrow \phi') \\
&= \int d\pi d\pi' \exp(-H(\phi, \pi)) P_M(\{\phi, \pi\} \rightarrow \{\phi', \pi'\}) P_A(\{\phi, \pi\} \rightarrow \{\phi', \pi'\}) \\
&= \int d\pi d\pi' \exp(-H(\phi', \pi')) P_M(\{\phi', -\pi'\} \rightarrow \{\phi, -\pi\}) P_A(\{\phi', \pi'\} \rightarrow \{\phi, \pi\}) \\
&= \int d(-\pi) d(-\pi') \exp(-H(\phi', -\pi')) P_M(\{\phi', -\pi'\} \rightarrow \{\phi, -\pi\}) P_A(\{\phi', -\pi'\} \rightarrow \{\phi, -\pi\}) \\
&= P_{\text{eq}}(\phi') P(\phi' \rightarrow \phi),
\end{aligned} \tag{226}$$

in which we used:

$$\begin{aligned}
&\exp(-H(\phi, \pi)) P_A(\{\phi, \pi\} \rightarrow \{\phi', \pi'\}) \\
&= \exp(-H(\phi, \pi)) \times \min\left(1, \exp(-H(\phi', \pi') + H(\phi, \pi))\right) \\
&= \begin{cases} \exp(-H(\phi, \pi)), & H(\phi', \pi') \leq H(\phi, \pi) \\ \exp(-H(\phi', \pi')), & H(\phi', \pi') > H(\phi, \pi) \end{cases};
\end{aligned} \tag{227}$$

$$\begin{aligned}
&\exp(-H(\phi', \pi')) P_A(\{\phi', \pi'\} \rightarrow \{\phi, \pi\}) \\
&= \exp(-H(\phi', \pi')) \times \min\left(1, \exp(H(\phi', \pi') - H(\phi, \pi))\right) \\
&= \begin{cases} \exp(-H(\phi', \pi')), & H(\phi, \pi) < H(\phi', \pi') \\ \exp(-H(\phi, \pi)), & H(\phi, \pi) \geq H(\phi', \pi') \end{cases};
\end{aligned} \tag{228}$$

$$\begin{aligned}
&\exp(-H(\phi, \pi)) P_A(\{\phi, \pi\} \rightarrow \{\phi', \pi'\}) \\
&= \exp(-H(\phi', \pi')) P_A(\{\phi', \pi'\} \rightarrow \{\phi, \pi\})
\end{aligned} \tag{229}$$

in the second equality.

5.2 Pseudofermion Method

We introduce the pseudofermion method to implement the MC method to simulate the lattice fermion fields. Here, we demonstrate this method from the following lattice theory

$$L_L = L_\phi + \sum_j \bar{\psi}_j D_\phi \psi_j, \quad (230)$$

in which L_ϕ is the Lagrangian for a lattice scalar field theory. The label ϕ in the D_ϕ indicates that the fermion field interacts with the scalar field. In general, integrating out fermion fields would give a non-positive definite determinant. The application of the MC simulation to a non-positive definite matrix cannot have the importance of sampling. We introduce the pseudofermion method for the case with the positive-definite determinant.

When considering two fermion fields as an example

$$\int \mathcal{D}\bar{\psi}\mathcal{D}\psi \exp(-\bar{\psi}_1 D\psi_1 - \bar{\psi}_2 D\psi_2) \sim \int \mathcal{D}\phi_{f,R}\mathcal{D}\phi_{f,I} \exp(-\phi_f^\dagger (DD^\dagger)^{-1}\phi_f), \quad (231)$$

where

$$\phi_f \equiv \phi_{f,R} + i\phi_{f,I}, \quad (232)$$

the DD^\dagger is a positive-definite matrix. We assume that the Dirac matrix satisfies the γ_5 -Hermiticity. Therefore, the determinant of D is equivalent to the determinant of D^\dagger . The ϕ_f is the bosonic field, and it is called the pseudofermionic field. We do not have Grassmann variables in the path integration, but we meet the non-local action.

The first step of implementation is to introduce the momenta π_j^* , π_j , and P_l canonically conjugate to $\phi_{f,j}^*$, $\phi_{f,j}$, and ϕ_l respectively. The Hamiltonian is

$$H = \frac{1}{2} \sum_l P_l^2 + \sum_j \pi_j^* \pi_j + S_\phi(\phi) + S_{pf}(\phi, \phi_f, \phi_f^*), \quad (233)$$

where

$$S_{pf} \equiv \sum_{j,k} \phi_{f,j}^* (Q^{-1})_{jk} \phi_{f,k}; \quad Q \equiv DD^\dagger. \quad (234)$$

The partition function is represented as follows

$$Z \equiv \int D\phi D\phi_f D\phi_f^* D P D\pi D\pi^* e^{-H}. \quad (235)$$

The following equations describe the molecular dynamics step:

$$\begin{aligned}
\dot{\phi}_l &= \frac{\partial H}{\partial P_l} = P_l; \\
\dot{P}_l &= -\frac{\partial H}{\partial \phi_l} = -\frac{\partial S_\phi}{\partial \phi_l} - \sum_{j,k} \phi_{f,j}^* \frac{\partial (Q^{-1})_{jk}}{\partial \phi_l} \phi_{f,k}; \\
\dot{\phi}_{f,j} &= \frac{\partial H}{\partial \pi_j^*} = \pi_j; \\
\dot{\pi}_j &= -\frac{\partial H}{\partial \phi_{f,j}^*} = -\sum_k (Q^{-1})_{jk} \phi_{f,k}.
\end{aligned} \tag{236}$$

The equation above can be simplified as follows:

$$\begin{aligned}
\eta_j &= \sum_k (Q^{-1})_{jk} \phi_{f,k}; \\
\dot{\phi}_{f,j} &= \pi_j; \\
\dot{\pi}_j &= -\eta_j; \\
\dot{\phi}_l &= P_l;
\end{aligned} \tag{237}$$

$$\dot{P}_l = -\frac{\partial S_\phi}{\partial \phi_l} + \sum_{j,k} \eta_j^* \frac{\partial Q_{jk}}{\partial \phi_l} \eta_k, \tag{238}$$

in which we used:

$$\begin{aligned}
0 &= \frac{\partial}{\partial \phi_l} (Q Q^{-1}) = \left(\frac{\partial}{\partial \phi_l} Q \right) Q^{-1} + Q \left(\frac{\partial}{\partial \phi_l} Q^{-1} \right); \\
\frac{\partial}{\partial \phi_l} Q^{-1} &= -Q^{-1} \left(\frac{\partial}{\partial \phi_l} Q \right) Q^{-1}
\end{aligned} \tag{239}$$

To perform the molecular dynamics practically, we rewrite the S_{pf} as below:

$$S_{pf} = \sum_{j,k} \phi_{f,j}^* ((D^\dagger)^{-1} D^{-1})_{jk} \phi_{f,k} = \sum_j \xi_j^* \xi_j, \tag{240}$$

where

$$\xi_j \equiv (D^{-1})_{jk} \phi_{f,k}. \tag{241}$$

Now, we can generate configurations in the variable ξ , which follow the Gaussian distribution. The value of ϕ_f can be calculated using the fixed configuration of the scalar field ϕ ,

$$\phi_f = D\xi. \tag{242}$$

An ensemble of configurations for the pseudofermionic variables with the distribution $\exp(-\phi_f^\dagger Q^{-1} \phi_f)$. When we generate the ξ with the Gaussian distribution, the simulation is unnecessary to generate π , and the pseudofermion field becomes a background field without the evolving of molecular dynamics. Indeed, this method is more practical. The algorithm of HMC is as in the following:

- 1. Choose an initial configuration for the scalar field ϕ .
- 2. Choose P_l from a Gaussian ensemble as

$$\exp\left(-\frac{1}{2} \sum_l P_l^2\right). \quad (243)$$

- 3. Choose ξ from the Gaussian distribution as $\exp(\xi^\dagger \xi)$.
- 4. Calculate

$$\phi_f = D\xi. \quad (244)$$

- 5. Allow the ϕ_l and its canonical momenta P_l to evolve according to:

$$\dot{\phi}_l = P_l; \quad (245)$$

$$\dot{P}_l = -\frac{\partial S_\phi}{\partial \phi_l} + \sum_{j,k} \eta_j^* \frac{\partial Q_{jk}}{\partial \phi_l} \eta_k, \quad (246)$$

where $\eta = Q^{-1} \phi_f$ with the fixed configuration of scalar field ϕ_f .

- 6. Accept the new configuration $(\tilde{\phi}, \tilde{P})$ with the probability

$$\min\left(1, \frac{\exp(-\tilde{H}[\tilde{\phi}, \tilde{P}])}{\exp(-\tilde{H}[\phi, P])}\right), \quad (247)$$

where

$$\tilde{H}[\phi, P] = \frac{1}{2} \sum_l P_l^2 + S_\phi[\phi] + \sum_j \xi_j^* \xi_j. \quad (248)$$

- 7. Save the configuration, whether new or old, based on the results of the Metropolis test.
- 8. Return to 2.

5.3 Box-Muller Method

We first give the algorithm for generating a random number with an arbitrary probability distribution and then apply it to the Gaussian distribution. A uniformly distributed random number is:

$$x \in [0, 1]; \quad x \equiv \int_{-\infty}^y dy P(y) \equiv F(y), \quad (249)$$

where $P(y)$ is a probability distribution. It is easy to know:

$$F(-\infty) = 0; \quad F(\infty) = 1. \quad (250)$$

The inverse F^{-1} gives

$$F^{-1}(x) = y(x). \quad (251)$$

Therefore, the variable x with a uniform distribution is equivalent to the variable y with a probability distribution $P(y)$:

$$\int dx = \int dy \frac{dx}{dy} = \int dy P(y). \quad (252)$$

The random numbers with Gaussian distribution

$$p(x) = \frac{1}{\sqrt{2\pi}} \exp\left(-\frac{x^2}{2}\right) \quad (253)$$

can be generated by the Box-Muller method. Consider points (x_1, x_2) in a plane where x_1 and x_2 both have Gaussian distribution:

$$p(x_1) = \frac{1}{\sqrt{2\pi}} \exp\left(-\frac{x_1^2}{2}\right), \quad p(x_2) = \frac{1}{\sqrt{2\pi}} \exp\left(-\frac{x_2^2}{2}\right). \quad (254)$$

Then the number of points in the $dx_1 dx_2$ is proportional to:

$$p(x_1)p(x_2)dx_1 dx_2 = \frac{1}{2\pi} e^{-\frac{x_1^2+x_2^2}{2}} dx_1 dx_2 = \frac{1}{2\pi} e^{-u} du d\theta, \quad (255)$$

where

$$x_1 \equiv \sqrt{2u} \cos(\theta), \quad x_2 = \sqrt{2u} \sin(\theta). \quad (256)$$

The variable $u \in (0, \infty)$ has an exponential distribution, and θ uniformly between 0 and 2π , and then both will have the desired Gaussian distribution. Hence, we have the following:

$$x = F(R) = \frac{1}{2\pi} \int_0^{2\pi} d\theta \int_0^{\frac{R^2}{2}} du e^{-u} = 1 - \exp\left(-\frac{R^2}{2}\right). \quad (257)$$

Because:

$$F(0) = 0; \quad F(\infty) = 1, \quad (258)$$

the x can be uniformly distributed on the unit interval $(0, 1)$. Therefore, we obtain:

$$R(x) = \sqrt{-2 \ln(1-x)} \equiv \sqrt{-2 \ln R_1}. \quad (259)$$

To generate the random variables, we choose:

$$R(x) \equiv \sqrt{-2 \ln R_1}; \quad \theta \equiv 2\pi R_2. \quad (260)$$

R_1 and R_2 are independent random numbers with a uniform distribution on the unit interval $(0, 1)$. Hence using:

$$x_1 = \sqrt{-2 \ln R_1} \cos(2\pi R_2); \quad x_2 = \sqrt{-2 \ln R_1} \sin(2\pi R_2) \quad (261)$$

shows the equivalence

$$\int dR_1 dR_2 = \frac{1}{2\pi} \int dx_1 dx_2 \exp\left(-\frac{x_1^2 + x_2^2}{2}\right). \quad (262)$$

5.4 Conjugate Gradient Method

The conjugate gradient method is an algorithm for obtaining x from the matrix equation

$$Ax = b \quad (263)$$

with a given positive-semidefinite matrix A and b . The idea is to minimize

$$S(x) = \frac{1}{2} |b - Ax|^2. \quad (264)$$

Assuming

$$x_{k+1} \equiv x_k + \lambda_k p_k, \quad (265)$$

the minimization of the $S(x)$ gives the condition:

$$\begin{aligned}
0 &= \frac{dS(x_{k+1})}{d\lambda_k} = \frac{1}{2} \frac{d}{d\lambda_k} |b - Ax_k - \lambda_k Ap_k|^2 \\
&\equiv \frac{1}{2} \frac{d}{d\lambda_k} (b - Ax_k - \lambda_k Ap_k, b - Ax_k - \lambda_k Ap_k) \\
&= \lambda_k (Ap_k, Ap_k) - (Ap_k, b - Ax_k),
\end{aligned} \tag{266}$$

which implies:

$$\lambda_k = \frac{(Ap_k, b - Ax_k)}{(Ap_k, Ap_k)} = \frac{(p_k, s_k)}{(Ap_k, Ap_k)}. \tag{267}$$

The s_k is defined by:

$$s_k \equiv A^\dagger r_k; \quad r_k \equiv b - Ax_k. \tag{268}$$

For an $n \times n$ matrix A ,

$$x = x_0 + \sum_{j=0}^{n-1} \lambda_j p_j, \tag{269}$$

in which p_0, p_1, \dots, p_{n-1} are linearly independent for $A^\dagger A$

$$(p_j, A^\dagger Ap_k) = 0 \tag{270}$$

for $j \neq k$. Now we assume

$$x_{j+1} \equiv x_0 + \sum_{k=0}^j \lambda_k p_k. \tag{271}$$

Therefore, this implies:

$$x_{k+1} = x_{j+1} + \sum_{l=j+1}^k \lambda_l p_l;$$

$$s_{k+1} = A^\dagger (b - Ax_{k+1}) = A^\dagger \left(b - Ax_{j+1} - \sum_{l=j+1}^k \lambda_l Ap_l \right) = s_{j+1} - \sum_{l=j+1}^k \lambda_l A^\dagger Ap_l;$$

$$\begin{aligned}
(p_j, s_{k+1}) &= (p_j, s_{j+1}) - \sum_{l=j+1}^k \lambda_l (p_j, A^\dagger Ap_l) = (p_j, s_{j+1}) = (p_j, A^\dagger (b - Ax_j - \lambda_j Ap_j)) \\
&= (p_j, s_j) - \lambda_j (Ap_j, Ap_j) = 0.
\end{aligned} \tag{272}$$

Now we choose

$$p_k = s_k + \mu_{k-1}p_{k-1}, \quad (273)$$

which leads to the following conditions:

$$0 = (p_{k-1}, A^\dagger Ap_k) = (p_{k-1}, A^\dagger As_k) + \mu_{k-1}(p_{k-1}, A^\dagger Ap_{k-1}). \quad (274)$$

Therefore, we obtain

$$\mu_{k-1} = -\frac{(p_{k-1}, A^\dagger As_k)}{(Ap_{k-1}, Ap_{k-1})}. \quad (275)$$

We first assume

$$(s_j, s_l) = 0, \quad j, l \leq k. \quad (276)$$

By using:

$$0 = (p_{k-1}, s_k) = (s_{k-1} + \mu_{k-2}p_{k-2}, s_k) = \mu_{k-2}(p_{k-2}, s_k), \quad (277)$$

the derivation can be done iterative, and it shows

$$(p_{j-1}, s_k) = 0, \quad j \leq k. \quad (278)$$

Hence, we obtain the:

$$0 = (p_j, s_{k+1}) = (s_j + \mu_{j-1}p_{j-1}, s_{k+1}) = (s_j, s_{k+1}), \quad (279)$$

which leads

$$(s_j, s_l) = 0, \quad j, l \leq k+1, \quad j \neq l. \quad (280)$$

We induce the above result from the assumption. Hence we prove

$$(s_j, s_l) = 0, \quad j \neq l. \quad (281)$$

Because the s_j are linearly independent, where

$$j = 0, 1, \dots, n-1, \quad (282)$$

it guarantees:

$$s_n = A^\dagger(b - Ax_n) = 0, \quad (283)$$

which implies

$$b - Ax_n = 0. \quad (284)$$

Hence, linear independence can guarantee finding a solution with suitable accuracy.

In the final, we show that the choice also guarantees

$$(p_j, A^\dagger Ap_l) = 0, \quad j \neq l. \quad (285)$$

We first obtain the below result:

$$(p_j, A^\dagger Ap_{l+1}) = (p_j, A^\dagger As_{l+1}) + \mu_l(p_j, A^\dagger Ap_l); \quad (286)$$

$$(p_j, A^\dagger As_{l+1}) = \frac{1}{\lambda_j}(x_{j+1} - x_j, A^\dagger As_{l+1}) = -\frac{1}{\lambda_j}(s_{j+1} - s_j, s_{l+1}) = 0, \quad (287)$$

in which we used:

$$A^\dagger A(x_{j+1} - x_j) = A^\dagger(- (b - Ax_{j+1}) + (b - Ax_j)) = A^\dagger(-r_{j+1} + r_j) = -s_{j+1} + s_j \quad (288)$$

in the second equality;

$$(p_j, A^\dagger Ap_{l+1}) = \mu_l(p_j, A^\dagger Ap_l), \quad j \neq l. \quad (289)$$

We first assume

$$(p_j, A^\dagger Ap_l) = 0, \quad j, l \leq k, \quad j \neq l. \quad (290)$$

Then this leads

$$(p_j, A^\dagger Ap_l) = 0, \quad j, l \leq k + 1, \quad j \neq l. \quad (291)$$

The induction proves

$$(p_j, A^\dagger Ap_l) = 0, \quad j \neq l. \quad (292)$$

Based on the above discussion, the algorithm of conjugate gradient is:

- Choosing an initial x_0 and then calculating

$$r_0 = b - Ax_0, \quad p_0 = s_0 = A^\dagger r_0.$$

- Repeating the below procedure for $k = 0, 1, \dots$:

$$\begin{aligned} \lambda_k &= \frac{(s_k, p_k)}{(Ap_k, Ap_k)}; \\ x_{k+1} &= x_k + \lambda_k p_k; \\ r_{k+1} &= b - Ax_{k+1}; \\ \text{If } |r_{k+1}| &< \epsilon, \text{ then stop;} \\ s_{k+1} &= A^\dagger r_{k+1}; \\ \mu_k &= -\frac{(p_k, A^\dagger A s_{k+1})}{(Ap_k, Ap_k)}; \\ p_{k+1} &= s_{k+1} + \mu_k p_k. \end{aligned}$$

Indeed, the above algorithm has unnecessary matrix calculation, but it is more intuitive. We will show some valuable identities for increasing the speed of the algorithm.

When we apply the conjugate gradient to solving a generic matrix, we solve the following positive-definite matrix $A^\dagger A$,

$$A^\dagger Ax \equiv Px = A^\dagger b \equiv \Phi. \quad (293)$$

Because the only difference is a multiplication of the A^\dagger , we still choose the minimization of the $S(x)$. Now we define:

$$R_k \equiv s_k = A^\dagger(b - Ax_k) = \Phi - Px_k. \quad (294)$$

Therefore, this gives:

$$(p_k, s_k) = (p_k, R_k) = (R_k + \mu_{k-1} p_{k-1}, R_k) = (R_k, R_k) + \mu_{k-1} (p_{k-1}, R_k). \quad (295)$$

Here we choose

$$p_k = R_k + \mu_{k-1} p_{k-1}. \quad (296)$$

We also have:

$$0 = (p_{k-1}, s_k) = (p_{k-1}, R_k). \quad (297)$$

Hence, we obtain the:

$$(p_k, s_k) = (R_k, R_k); \quad \lambda_k = \frac{(R_k, R_k)}{(p_k, Pp_k)}. \quad (298)$$

Due to the fact:

$$R_{k+1} - R_k = P(x_k - x_{k+1}) = -\lambda_k Pp_k, \quad (299)$$

it gives:

$$\begin{aligned} (R_{k+1}, R_{k+1}) &= (R_{k+1}, R_k) - \lambda_k (R_{k+1}, Pp_k) \\ &= (R_{k+1}, R_k) - \frac{(R_k, R_k)}{(P_k, Pp_k)} (R_{k+1}, Pp_k). \end{aligned} \quad (300)$$

Hence we obtain

$$(R_{k+1}, R_{k+1}) = -\frac{(R_k, R_k)}{(P_k, Pp_k)} (R_{k+1}, Pp_k) \quad (301)$$

from

$$0 = (s_{k+1}, s_k) = (R_{k+1}, R_k). \quad (302)$$

The μ_k is

$$\mu_k = \frac{(R_{k+1}, R_{k+1})}{(R_k, R_k)}. \quad (303)$$

The algorithm is:

- Choosing an initial x_0 and then calculating:

$$R_0 = \Phi - Px_0, \quad p_0 = R_0, \quad k = 0.$$

- Repeating the following procedure for $k = 0, 1, \dots$:

$$\begin{aligned} \lambda_k &= \frac{(R_k, R_k)}{(p_k, Pp_k)}; \\ R_{k+1} &= R_k - \lambda_k Pp_k; \\ \text{If } |R_{k+1}| &< \epsilon|\Phi|, \text{ then stop;} \\ \mu_k &= \frac{(R_{k+1}, R_{k+1})}{(R_k, R_k)}; \\ x_{k+1} &= x_k + \lambda_k p_k; \\ p_{k+1} &= R_{k+1} + \mu_k p_k. \end{aligned}$$

This algorithm is more efficient.

5.5 Non-Hermitian Lattice Formulation

Applying the HMC method to the non-Hermitian lattice formulation is problematic because it loses the Hermiticity. Implementing the Monte Carlo method only requires the non-negative partition function. We demonstrate our simulation from 1D Dirac fermion fields with a degenerate mass for two flavors [27]

$$S_{\text{FD}} = a \sum_{n=0}^{N-1} \left(\bar{\psi}_1(n)(D(n) + m_{\text{F}})\psi_1(n) + \bar{\psi}_2(n)(-D^\dagger(n) + m_{\text{F}})\psi_2(n) \right). \quad (304)$$

The forward finite-difference defines the derivative operator of ψ_1 , and the derivative operator of another field ψ_2 is defined using the backward finite-difference. After integrating out the fermion fields, we obtain a non-negative partition function [27]:

$$\begin{aligned} \det(D + m) \det(-D^\dagger + m_{\text{F}}) &= \det(D + m_{\text{F}}) \det(\gamma_5(-D^\dagger + m_{\text{F}})\gamma_5) \\ &= |\det(D + m_{\text{F}})|^2. \end{aligned} \quad (305)$$

We use

$$\gamma_5 D + D \gamma_5 = 0 \quad (306)$$

in the second equality. We then introduce the pseudo-fermion field (bosonic field ϕ_f) to rewrite the partition function as in the following

$$\begin{aligned} &\int \mathcal{D}\bar{\psi} \mathcal{D}\psi \exp(-S_{\text{FD}}) \\ &\sim \int \mathcal{D}\phi_{f,\text{R}} \mathcal{D}\phi_{f,\text{I}} \exp\left(-\phi_f^\dagger ((D + m_{\text{F}})(D^\dagger + m_{\text{F}}))^{-1} \phi_f\right), \end{aligned} \quad (307)$$

where

$$\phi_f \equiv \phi_{f,\text{R}} + i\phi_{f,\text{I}}. \quad (308)$$

Although it is a non-Hermitian field theory, the partition function is real-valued. Hence, we can implement the HMC method to compute the observables [27]. This method can have a similar extension to the even flavors and also the interacting theory [28].

6 Chiral Anomaly and Index Theorem

The chiral anomaly can be introduced through the chiral transformation applied to the measure [19]. This method can also be implemented on a lattice [20, 22]. The

chiral anomaly is relevant to the index theorem [15, 16, 17] or the topological charge [19]. Hence, we can apply the technique to realize the index theorem on a lattice [20, 22]. However, the chiral anomaly on a lattice indicates topologically nontrivial background gauge fields, even if the topological charge is zero [24, 25]. Hence, the non-trivial topological charge should rely on a non-trivially infinite lattice size limit [24, 25]. We provide one solution of the Ginsparg-Wilson relation to explain such a situation [8, 24, 25].

6.1 Chiral Anomaly

Consider the functional integral for massless Dirac fermions coupled to a gauge field A_μ ,

$$Z = \int [d\psi d\bar{\psi}] e^{-S(\psi, \bar{\psi})}, \quad (309)$$

where

$$S(\psi, \bar{\psi}) = \int d^4x \bar{\psi} \gamma_\mu (\partial_\mu + A_\mu) \psi. \quad (310)$$

This classical action has chiral symmetry. We now consider a change of variables

$$\tilde{\psi} = e^{i\gamma_5 \alpha(x)} \psi, \quad \tilde{\bar{\psi}} = \bar{\psi} e^{i\gamma_5 \alpha(x)}, \quad (311)$$

where $\alpha(x)$ is defined as an arbitrary function of the coordinates. Because it is just a change of variables, the partition function Z is unchanged [19]:

$$\begin{aligned} Z &= \int [d\tilde{\psi} d\tilde{\bar{\psi}}] e^{-S(\tilde{\psi}, \tilde{\bar{\psi}})} = \int [d\psi d\bar{\psi}] \det(e^{2i\gamma_5 \alpha}) e^{-S(\psi, \bar{\psi})} \exp\left(-\int d^4x \alpha \partial_\mu J_\mu\right) \\ &= \int [d\psi d\bar{\psi}] e^{-S(\psi, \bar{\psi})} \exp\left(2i \text{Tr}(\gamma_5 \alpha) - \int d^4x \alpha \partial_\mu J_\mu\right), \end{aligned} \quad (312)$$

where

$$J_\mu = i\bar{\psi} \gamma_\mu \gamma_5 \psi. \quad (313)$$

The trace operation is over the infinite-dimensional spaces of eigenmodes and the Dirac matrices. Since the measure is not invariant under chiral transformations, chiral symmetry is broken due to quantum effects [19].

6.2 Topological Charge

After performing the trace operation $\text{Tr}(\gamma_5)$, we can discover that the chiral anomaly can be relevant to the index theorem or the topological charge. The non-zero eigenvalues and their corresponding eigenmodes are paired, meaning they will effectively cancel each other out. We only need to be concerned about the zero eigenvalues. Therefore, we can introduce the regulator Λ and extract the result when $\Lambda \rightarrow \infty$,

$$\begin{aligned}
\text{Tr}(\gamma_5) &= \lim_{\Lambda^2 \rightarrow \infty} \text{Tr} \left(\gamma_5 e^{\frac{\gamma_\mu (\partial_\mu + A_\mu)}{\Lambda^2}} \right) \\
&= \int \frac{d^4 p}{(2\pi)^4} \text{Tr} \left(\langle y|p\rangle \langle p|\gamma_5 e^{-\frac{(\gamma_\mu (p_\mu - iA_\mu))^2}{\Lambda^2}} |x\rangle \right)_{\Lambda^2 \rightarrow \infty, y \rightarrow x} \\
&= \lim_{\Lambda^2 \rightarrow \infty} \left[\int d^4 x \text{Tr} \left(\frac{1}{8M^4} \gamma_5 F_{\mu\nu} \gamma_\mu \gamma_\nu F_{\rho\sigma} \gamma_\rho \gamma_\sigma \right) \int \frac{d^4 p}{(2\pi)^4} e^{-\frac{p^2}{\Lambda^2}} \right] \\
&= \frac{1}{16\pi^2} \int d^4 x \epsilon_{\mu\nu\rho\sigma} \text{Tr}(F_{\mu\nu} F_{\rho\sigma}), \tag{314}
\end{aligned}$$

where the field strength $F_{\mu\nu}$ is defined as

$$F_{\mu\nu} \equiv \partial_\mu A_\nu - \partial_\nu A_\mu + [A_\mu, A_\nu]. \tag{315}$$

We use the convention:

$$\epsilon_{0123} = 1; \quad \text{Tr}(\gamma^5 \gamma^\mu \gamma^\nu \gamma^\rho \gamma^\sigma) = 4\epsilon^{\mu\nu\rho\sigma} \tag{316}$$

and the following identity:

$$\gamma^\mu \gamma^\nu \mathcal{D}_\mu \mathcal{D}_\nu = \frac{1}{2} \{\gamma_\mu, \gamma_\nu\} \mathcal{D}_\mu \mathcal{D}_\nu + \frac{1}{2} [\gamma_\mu, \gamma_\nu] \mathcal{D}_\mu \mathcal{D}_\nu = \mathcal{D}^2 + \frac{1}{2} \gamma_\mu \gamma_\nu F_{\mu\nu}, \tag{317}$$

where \mathcal{D}_μ is the covariant derivative

$$\mathcal{D}_\mu \equiv \partial_\mu + A_\mu. \tag{318}$$

The results show that $\text{Tr}(\gamma_5)$ induces the topological charge. Therefore, it reflects that the topological charge density induces the chiral anomaly (or the non-conservation of the current).

6.3 Index Theorem on Lattice

When a Dirac matrix satisfies the Ginsparg-Wilson relation [8]

$$\gamma_5 D + \gamma_5 = a D \gamma_5 D, \tag{319}$$

the lattice artifact modifies the chiral transformation [9]:

$$\psi \rightarrow \exp \left[i\alpha \gamma_5 \left(1 - \frac{a}{2} D \right) \right] \psi; \quad \bar{\psi} \rightarrow \bar{\psi} \exp \left[i\alpha \left(1 - \frac{a}{2} D \right) \gamma_5 \right]. \quad (320)$$

The chiral anomaly is also modified, and then the index theorem is realized through the expression [19]:

$$\text{Tr} \left[\gamma_5 \left(1 - \frac{a}{2} D \right) \right] = \frac{1}{2} \sum_{\lambda} (v_{\lambda}, \gamma_5 (2 - aD) v_{\lambda}) = \frac{1}{2} \sum_{\lambda} (2 - a\lambda) (v_{\lambda}, \gamma_5 v_{\lambda}) = n_+ - n_-, \quad (321)$$

where a is the lattice spacing, v_{λ} is an eigenvector of D associated with the eigenvalue λ , and n_+ and n_- denote the number of left- and right-handed zero modes. Only eigenvectors with real eigenvalues, 0 and $2/a$, have the non-vanishing chirality [19]:

$$(v_{\lambda=0}, \gamma_5 v_{\lambda=0}) \neq 0; \quad (v_{\lambda=\frac{2}{a}}, \gamma_5 v_{\lambda=\frac{2}{a}}) \neq 0. \quad (322)$$

The topological charge is significantly influenced only by the zero modes [19].

When a Dirac matrix satisfies

$$\gamma_5 D + D \gamma_5 = 0, \quad (323)$$

the chiral anomaly is only contributed from $\text{Tr}(\gamma_5)$. When tracing over the Dirac indices first, it shows zero already. On a finite lattice, there is no chiral anomaly. However, it is difficult to say that the lattice fermion theory is inconsistent due to the loss of the anomaly on a finite lattice. We will give one example, showing that the topologically-nontrivial background gauge fields always possess zero topological charge on a finite lattice [24, 25]. This example teaches us that it is tricky from the infinite lattice size limit [24, 25]. The loss of the chiral anomaly is likely due to the consideration of a finite lattice. The physical observable can still be obtained from the lattice simulation [24, 25].

6.4 Zero Mode and Chiral Anomaly

The Dirac operator is defined as follows [24, 25]

$$D = \frac{1}{a} D_c \left(1 + \frac{1}{2} D_c \right)^{-1}, \quad (324)$$

where

$$\gamma_5 D_c + D_c \gamma_5 = 0, \quad (325)$$

we can use

$$D^{-1} = a \left(\frac{1}{2} + D_c^{-1} \right) \quad (326)$$

to show the Ginsparg-Wilson relation or [24, 25]

$$\gamma_5 D^{-1} + D^{-1} \gamma_5 = a \gamma_5. \quad (327)$$

This Dirac matrix satisfies the γ_5 -Hermiticity [24, 25]. The zero mode of the Dirac matrix is also a zero mode of D_c [24, 25]. Suppose the spectrum of D_c does not contain any poles for a topologically-nontrivial gauge background. In that case, the Dirac matrix loses topological zero modes. The solution with properties that are exponentially local, free of doublers, and exhibit expected continuum behavior was constructed in Ref. [24]. Due to the loss of the topological zero modes, the topological charge is zero even if the chiral anomaly appears [24, 25]. The homogeneous part of the topological charge density (contributing to the zero topological charge) is recovered in the infinite lattice size and continuum limits as the expected result [24, 25]. Hence, the winding part of the topological charge density (contributing to the non-zero topological charge) is suppressed when the lattice size approaches infinity [24, 25]. To have the non-trivial contribution of the topological charge, we should carefully treat the infinite summation of the infinitesimal value. Due to similar issues with anomaly calculation, assessing consistency at a finite lattice level is challenging.

7 Outlook and Future Directions

We identified the challenges and trade-offs in putting chiral fermions on the lattice, particularly regarding chiral symmetry and Hermiticity. The Nielsen-Ninomiya theorem constrains the possibilities for chiral fermions on a lattice [4, 5]. Typical methods, like Wilson [1] and overlap fermions [6], circumvented the theorem at the cost of local action. Non-Hermitian formulations stood out here as they sidestep the no-go theorem by abandoning Hermiticity [11], allowing for both chiral symmetry and local action—though this introduces other technical issues for simulation.

The usage of even-flavor fermions as a means to achieve a positive-definite partition function is a significant workaround [27]. It allows MC simulations in the non-Hermitian lattice formulation [27]. While the exact chiral symmetry in non-Hermitian setups challenges traditional views on the chiral anomaly on the lattice [27], this could still be resolved or recovered in the infinite-volume limit. This area remains open and intriguing for further exploration, especially regarding how the anomaly behavior adjusts in the infinite-volume limit.

This area in finite-density QCD is complex yet essential, as the sign problem prevents standard Monte Carlo simulations at a real chemical potential. Using imaginary chemical potential and analytical continuation is one of the few viable approaches, and combining it with a lattice formulation that respects exact chiral symmetry can provide a significant advantage. Resummation methods can be potent here, allowing us to explore non-perturbative effects and, ideally, to verify results from lattice simulations in strong coupling regimes. Matching these two methods offers robust insights into QCD's phase transitions and other phenomena.

Focusing on low-lying eigenmodes for non-Hermitian lattice QCD could streamline simulations while retaining physical insights, especially in the absence of zero modes. This selective approach could reveal whether low-mode truncations approximate the continuum results within acceptable tolerances, particularly for observables sensitive to chiral symmetry breaking or confinement. Establishing an efficient method is meaningful. Because the Dirac matrix does not possess the zero modes [27], more consistent checks between the lattice simulation and the continuum field theory should confirm whether the topologically trivial configurations could reproduce physical results [24, 25].

Acknowledgments

We want to express our gratitude to Sinya Aoki, Xing Huang, and Hersh Singh for their helpful discussion. CTM would like to thank Nan-Peng Ma for his encouragement. CTM acknowledges the Nuclear Physics Quantum Horizons program through the Early Career Award (Grant No. DE-SC0021892); YST Program of the APCTP; China Postdoctoral Science Foundation, Postdoctoral General Funding: Second Class (Grant No. 2019M652926). HZ acknowledges the Guangdong Major Project of Basic and Applied Basic Research (Grant No. 2020B0301030008); the Science and Technology Program of Guangzhou (Grant No. 2019050001); the National Natural Science

Foundation of China (Grants No. 12047523 and 12105107).

References

- [1] K. G. Wilson, “Confinement of Quarks,” *Phys. Rev. D* **10**, 2445-2459 (1974)
doi:10.1103/PhysRevD.10.2445
- [2] J. S. Schwinger, “On the Green’s functions of quantized fields. 1.,” *Proc. Nat. Acad. Sci.* **37**, 452-455 (1951) doi:10.1073/pnas.37.7.452
- [3] M. Gell-Mann and F. E. Low, “Quantum electrodynamics at small distances,” *Phys. Rev.* **95**, 1300-1312 (1954) doi:10.1103/PhysRev.95.1300
- [4] H. B. Nielsen and M. Ninomiya, “Absence of Neutrinos on a Lattice. 1. Proof by Homotopy Theory,” *Nucl. Phys. B* **185**, 20 (1981) [erratum: *Nucl. Phys. B* **195**, 541 (1982)] doi:10.1016/0550-3213(82)90011-6
- [5] H. B. Nielsen and M. Ninomiya, “Absence of Neutrinos on a Lattice. 2. Intuitive Topological Proof,” *Nucl. Phys. B* **193**, 173-194 (1981) doi:10.1016/0550-3213(81)90524-1
- [6] H. Neuberger, “More about exactly massless quarks on the lattice,” *Phys. Lett. B* **427**, 353-355 (1998) doi:10.1016/S0370-2693(98)00355-4 [arXiv:hep-lat/9801031 [hep-lat]].
- [7] L. H. Karsten, “Lattice Fermions in Euclidean Space-time,” *Phys. Lett. B* **104**, 315-319 (1981) doi:10.1016/0370-2693(81)90133-7
- [8] P. H. Ginsparg and K. G. Wilson, “A Remnant of Chiral Symmetry on the Lattice,” *Phys. Rev. D* **25**, 2649 (1982) doi:10.1103/PhysRevD.25.2649
- [9] M. Luscher, “Exact chiral symmetry on the lattice and the Ginsparg-Wilson relation,” *Phys. Lett. B* **428**, 342-345 (1998) doi:10.1016/S0370-2693(98)00423-7 [arXiv:hep-lat/9802011 [hep-lat]].

- [10] P. Hernandez, K. Jansen and M. Luscher, “Locality properties of Neuberger’s lattice Dirac operator,” Nucl. Phys. B **552**, 363-378 (1999) doi:10.1016/S0550-3213(99)00213-8 [arXiv:hep-lat/9808010 [hep-lat]].
- [11] I. O. Stamatescu and T. T. Wu, “A New formulation of lattice gauge theory with fermions,” CERN-TH-6631-92.
- [12] J. B. Kogut and L. Susskind, “Hamiltonian Formulation of Wilson’s Lattice Gauge Theories,” Phys. Rev. D **11**, 395-408 (1975) doi:10.1103/PhysRevD.11.395
- [13] M. Creutz, I. Horvath and H. Neuberger, “A New fermion Hamiltonian for lattice gauge theory,” Nucl. Phys. B Proc. Suppl. **106**, 760-762 (2002) doi:10.1016/S0920-5632(01)01836-9 [arXiv:hep-lat/0110009 [hep-lat]].
- [14] T. Hayata, K. Nakayama and A. Yamamoto, “Chiral fermion in the Hamiltonian lattice gauge theory,” Phys. Rev. D **108**, no.3, 034511 (2023) doi:10.1103/PhysRevD.108.034511 [arXiv:2305.18934 [hep-lat]].
- [15] M. F. Atiyah and I. M. Singer, “The Index of elliptic operators. 1,” Annals Math. **87**, 484-530 (1968) doi:10.2307/1970715
- [16] M. F. Atiyah and I. M. Singer, “The Index of elliptic operators. 4,” Annals Math. **93**, 119-138 (1971) doi:10.2307/1970756
- [17] M. F. Atiyah and I. M. Singer, “The Index of elliptic operators. 5.,” Annals Math. **93**, 139-149 (1971) doi:10.2307/1970757
- [18] P. Hasenfratz, V. Laliena and F. Niedermayer, “The Index theorem in QCD with a finite cutoff,” Phys. Lett. B **427**, 125-131 (1998) doi:10.1016/S0370-2693(98)00315-3 [arXiv:hep-lat/9801021 [hep-lat]].
- [19] K. Fujikawa, “Path Integral Measure for Gauge Invariant Fermion Theories,” Phys. Rev. Lett. **42**, 1195-1198 (1979) doi:10.1103/PhysRevLett.42.1195

- [20] K. Fujikawa, “A Continuum limit of the chiral Jacobian in lattice gauge theory,” Nucl. Phys. B **546**, 480-494 (1999) doi:10.1016/S0550-3213(99)00042-5 [arXiv:hep-th/9811235 [hep-th]].
- [21] D. H. Adams, “Axial anomaly and topological charge in lattice gauge theory with overlap Dirac operator,” Annals Phys. **296**, 131-151 (2002) doi:10.1006/aphy.2001.6209 [arXiv:hep-lat/9812003 [hep-lat]].
- [22] H. Suzuki, “Simple evaluation of chiral Jacobian with overlap Dirac operator,” Prog. Theor. Phys. **102**, 141-147 (1999) doi:10.1143/PTP.102.141 [arXiv:hep-th/9812019 [hep-th]].
- [23] T. W. Chiu, “The Spectrum and topological charge of exactly massless fermions on the lattice,” Phys. Rev. D **58**, 074511 (1998) doi:10.1103/PhysRevD.58.074511 [arXiv:hep-lat/9804016 [hep-lat]].
- [24] T. W. Chiu, “The Index of a Ginsparg-Wilson Dirac operator,” Phys. Lett. B **521**, 429-433 (2001) doi:10.1016/S0370-2693(01)01222-9 [arXiv:hep-lat/0106012 [hep-lat]].
- [25] T. W. Chiu and T. H. Hsieh, “A Perturbative calculation of the axial anomaly of a Ginsparg-Wilson Dirac operator,” Phys. Rev. D **65**, 054508 (2002) doi:10.1103/PhysRevD.65.054508 [arXiv:hep-lat/0109016 [hep-lat]].
- [26] N. Sadooghi and H. J. Rothe, “Continuum behavior of lattice QED, discretized with one sided lattice differences, in one loop order,” Phys. Rev. D **55**, 6749-6759 (1997) doi:10.1103/PhysRevD.55.6749 [arXiv:hep-lat/9610001 [hep-lat]].
- [27] X. Guo, C. T. Ma and H. Zhang, “Naive lattice fermion without doublers,” Phys. Rev. D **104**, no.9, 094505 (2021) doi:10.1103/PhysRevD.104.094505 [arXiv:2105.10977 [hep-lat]].

- [28] X. Guo, C. T. Ma and H. Zhang, “Non-Hermitian lattice fermions in the 2D Gross-Neveu-Yukawa model,” *Phys. Rev. D* **110**, no.3, 034502 (2024) doi:10.1103/PhysRevD.110.034502 [arXiv:2404.18441 [hep-th]].
- [29] B. B. Brandt, G. Endrodi and S. Schmalzbauer, “QCD phase diagram for nonzero isospin-asymmetry,” *Phys. Rev. D* **97**, no.5, 054514 (2018) doi:10.1103/PhysRevD.97.054514 [arXiv:1712.08190 [hep-lat]].
- [30] W. Q. Chen, Y. S. Wu, W. Xi, W. Z. Yi and G. Yue, “Fate of Quantum Anomalies for 1d lattice chiral fermion with a simple non-Hermitian Hamiltonian,” *JHEP* **05**, 090 (2023) doi:10.1007/JHEP05(2023)090 [arXiv:2010.09375 [cond-mat.other]].
- [31] T. Bessho and M. Sato, “Nielsen-Ninomiya Theorem with Bulk Topology: Duality in Floquet and Non-Hermitian Systems,” *Phys. Rev. Lett.* **127**, no.19, 196404 (2021) doi:10.1103/PhysRevLett.127.196404 [arXiv:2006.04204 [cond-mat.mes-hall]].
- [32] M. Aizenman, “Proof of the Triviality of ϕ^4 in D-Dimensions Field Theory and Some Mean Field Features of Ising Models for $D > 4$,” *Phys. Rev. Lett.* **47**, 1-4 (1981) doi:10.1103/PhysRevLett.47.1
- [33] M. Luscher and P. Weisz, “Scaling Laws and Triviality Bounds in the Lattice ϕ^4 Theory. 1. One Component Model in the Symmetric Phase,” *Nucl. Phys. B* **290**, 25-60 (1987) doi:10.1016/0550-3213(87)90177-5
- [34] D. J. Gross and F. Wilczek, “Ultraviolet Behavior of Nonabelian Gauge Theories,” *Phys. Rev. Lett.* **30**, 1343-1346 (1973) doi:10.1103/PhysRevLett.30.1343
- [35] H. D. Politzer, “Reliable Perturbative Results for Strong Interactions?,” *Phys. Rev. Lett.* **30**, 1346-1349 (1973) doi:10.1103/PhysRevLett.30.1346
- [36] W. E. Thirring, “A Soluble relativistic field theory?,” *Annals Phys.* **3**, 91-112 (1958) doi:10.1016/0003-4916(58)90015-0

- [37] T. H. R. Skyrme, “A Nonlinear theory of strong interactions,” Proc. Roy. Soc. Lond. A **247**, 260-278 (1958) doi:10.1098/rspa.1958.0183
- [38] T. H. R. Skyrme, “Particle states of a quantized meson field,” Proc. Roy. Soc. Lond. A **262**, 237-245 (1961) doi:10.1098/rspa.1961.0115
- [39] S. R. Coleman, “The Quantum Sine-Gordon Equation as the Massive Thirring Model,” Phys. Rev. D **11**, 2088 (1975) doi:10.1103/PhysRevD.11.2088
- [40] S. Mandelstam, “Soliton Operators for the Quantized Sine-Gordon Equation,” Phys. Rev. D **11**, 3026 (1975) doi:10.1103/PhysRevD.11.3026
- [41] T. H. Buscher, “A Symmetry of the String Background Field Equations,” Phys. Lett. B **194**, 59-62 (1987) doi:10.1016/0370-2693(87)90769-6
- [42] T. H. Buscher, “Path Integral Derivation of Quantum Duality in Nonlinear Sigma Models,” Phys. Lett. B **201**, 466-472 (1988) doi:10.1016/0370-2693(88)90602-8
- [43] C. P. Burgess and F. Quevedo, “Bosonization as duality,” Nucl. Phys. B **421**, 373-390 (1994) doi:10.1016/0550-3213(94)90332-8 [arXiv:hep-th/9401105 [hep-th]].
- [44] J. Kovacs, S. Nagy and K. Sailer, “Asymptotic safety in the sine-Gordon model,” Phys. Rev. D **91**, no.4, 045029 (2015) doi:10.1103/PhysRevD.91.045029 [arXiv:1408.2680 [hep-th]].
- [45] C. T. Ma, Y. Pan and H. Zhang, “Explore the Origin of Spontaneous Symmetry Breaking from Adaptive Perturbation Method,” JHAP **4**, no.1, 51-64 (2024) doi:10.22128/JHAP.2024.754.1066 [arXiv:2205.00414 [hep-th]].
- [46] C. T. Ma and H. Zhuang, “Study of asymptotic free scalar field theories from adaptive perturbation method,” Annals Phys. **472**, 169856 (2025) doi:10.1016/j.aop.2024.169856 [arXiv:2305.05266 [hep-th]].